




5-2020

## Immobilization of Phosphotungstic Acid on Silica Surface for Catalytic Alkylation of Aromatic Compounds

Anastasia Kuvayskaya  
*East Tennessee State University*

Follow this and additional works at: <https://dc.etsu.edu/etd>

 Part of the [Environmental Chemistry Commons](#), [Materials Chemistry Commons](#), and the [Organic Chemistry Commons](#)

---

### Recommended Citation

Kuvayskaya, Anastasia, "Immobilization of Phosphotungstic Acid on Silica Surface for Catalytic Alkylation of Aromatic Compounds" (2020). *Electronic Theses and Dissertations*. Paper 3738. <https://dc.etsu.edu/etd/3738>

This Thesis - unrestricted is brought to you for free and open access by the Student Works at Digital Commons @ East Tennessee State University. It has been accepted for inclusion in Electronic Theses and Dissertations by an authorized administrator of Digital Commons @ East Tennessee State University. For more information, please contact [digilib@etsu.edu](mailto:digilib@etsu.edu).

Immobilization of Phosphotungstic Acid on Silica Surface for Catalytic Alkylation of Aromatic  
Compounds

---

A thesis

presented to

the faculty of the Department of Chemistry

East Tennessee State University

In partial fulfillment

of the requirements for the degree

Master of Science in Chemistry

---

by

Anastasia Kuvayskaya

May 2020

---

Dr. Aleksey Vasiliev, Chair

Dr. Greg Bishop

Dr. Abbas Shilabin

Keywords: Phosphotungstic acid, sol-gel synthesis, catalyst, alkylbenzenes

## ABSTRACT

Immobilization of Phosphotungstic Acid on Silica Surface for Catalytic Alkylation of Aromatic Compounds

by

Anastasia Kuvayskaya

Superacidic mesoporous materials containing covalently embedded PTA were synthesized by sol-gel method. Tetraethyl orthosilicate (TEOS) and phosphotungstic acid (PTA) were used as precursors in the synthesis, ionic and nonionic surfactants were used as pore-forming agents, the reaction proceeded in acidic media. TEM images revealed mesoporous structure with embedded PTA clusters. FT-IR spectra of obtained materials contained characteristic bands of PTA at  $957\text{ cm}^{-1}$ . Synthesized catalysts had high BET surface area and high concentration of acidic sites. Alkylation of 1,3,5-trimethylbenzene by 1-decene demonstrated high catalytic activity. The catalyst obtained with Pluronic P123 as a template was the most effective and resulted in highest conversion of 1-decene into alkylated products. Covalent embedding of PTA clusters in addition to thermal and chemical stability of synthesized catalysts enabled their recyclability. Catalysts remained active during subsequent cycles of alkylation.

Copyright 2020 by Anastasia Kuvayskaya  
All Rights Reserved

## DEDICATION

This work is dedicated to my husband Sam Cox, my son Dominic Hartz, my parents Emma Kim and Aleksey Kuvayskiy and my brother Dima Kuvayskiy.

## ACKNOWLEDGEMENTS

I would like to express the sincerest gratitude to my advisor Dr. Vasiliev for his mentorship, patience, understanding and guidance during my pursuit of master's degree in chemistry. I could not have asked for a better mentor.

I am extremely grateful to Dr. Mohseni for all his help with the use of instrumentation and willingness to answer multiple questions I had while working on my project.

I would like to express sincere appreciation to Dr. Bishop and Dr. Shilabin for serving as committee members for my thesis.

Thank you, Maria Kalis, for helping me to navigate organizational and administrative aspects during my journey through graduate school.

This research was supported by the Donors of the American Chemical Society Petroleum Research Fund.

## TABLE OF CONTENTS

|                                      |    |
|--------------------------------------|----|
| ABSTRACT.....                        | 2  |
| DEDICATION.....                      | 4  |
| ACKNOWLEDGEMENTS.....                | 5  |
| LIST OF TABLES.....                  | 9  |
| LIST OF FIGURES.....                 | 10 |
| LIST OF ABBREVIATIONS.....           | 12 |
| CHAPTER 1. INTRODUCTION.....         | 13 |
| Alkylated Benzenes.....              | 13 |
| Zeolites.....                        | 16 |
| Heteropolyacids.....                 | 19 |
| Sol-Gel Method.....                  | 21 |
| Mesoporous Materials.....            | 24 |
| Surfactants.....                     | 25 |
| Research Objectives.....             | 26 |
| CHAPTER 2. EXPERIMENTAL METHODS..... | 28 |
| Reagents Used.....                   | 28 |
| Synthetic Procedures.....            | 29 |
| Instrumental Characterization.....   | 30 |

|   |    |
|---|----|
| Elemental Analysis.....                               | 30 |
| Surface Acidity.....                                  | 30 |
| Fourier-Transform Infrared (FT-IR) Spectroscopy.....  | 31 |
| Transmission Electron Microscopy (TEM) .....          | 31 |
| Porosity .....  | 31 |
| Thermoanalysis .....                                  | 31 |
| Alkylation of 1,3,5-Trimethylbenzene by 1-Decene..... | 32 |
| Procedure.....  | 32 |
| GC-MS Analysis .....                                  | 32 |
| CHAPTER 3. RESULTS.....                               | 34 |
| Synthesis and Chemical Composition.....               | 34 |
| Synthesis .....                                       | 34 |
| Content of Immobilized Heteropolyacid.....            | 34 |
| Surface Acidity.....                                  | 34 |
| Structural Characteristics .....                      | 36 |
| Fourier-Transform Infrared (FT-IR) Spectroscopy.....  | 36 |
| Transmission Electron Microscopy (TEM) .....          | 37 |
| Particle Size.....                                    | 37 |
| Porosity .....  | 38 |
| Thermoanalysis .....                                  | 39 |



|   |    |
|---|----|
| Catalytic Activity .....  | 40 |
| Effect of Temperature .....                                     | 40 |
| Effect of HCl Concentration .....                               | 41 |
| Isomeric Composition of Alkylated 1,3,5-Trimethylbenzenes ..... | 43 |
| Recycling of the Catalyst .....                                 | 46 |
| CHAPTER 4. DISCUSSION.....                                      | 47 |
| Characteristics of the Catalysts .....                          | 47 |
| Catalytic Properties .....                                      | 49 |
| Conclusions .....   | 51 |
| REFERENCES .....  | 52 |
| VITA.....   | 59 |

## LIST OF TABLES

|  |    |
|--|----|
| Table 1. Chemicals used .....  | 28 |
| Table 2. Characteristics of the catalysts.....   | 35 |
| Table 3. Catalytic activity .....  | 42 |
| Table 4. Isomeric alkylbenzenes formed on catalyst <b>1</b> at 140°C .....   | 45 |
| Table 5. Characteristics of <b>1</b> after initial ( <b>1</b> ) and subsequent ( <b>1-R</b> ) round of alkylation..... | 46 |

## LIST OF FIGURES AND SCHEMES

|  |    |
|--|----|
| Figure 1. General LAS structure.....   | 13 |
| Figure 2. Micropore system and general structure of four zeolites .....  | 17 |
| Figure 3. Representation of a generic Keggin structure. ....   | 20 |
| Figure 4. Monomeric silica addition (mechanism 1). Formation of ordered mesoporous structure<br>by aggregation (mechanism 2). .... | 24 |
| Figure 5. Non-ionic surfactant, PEG-PPG-PEG (Pluronic).....  | 26 |
| Figure 6. Anionic surfactant, dodecyltrimethylammonium chloride.....   | 26 |
| Figure 7. Cationic surfactant, sodium dodecyl sulfate.....   | 26 |
| Figure 8. Synthesis of mesoporous materials by sol-gel method.....   | 29 |
| Figure 9. 1,3,5-Trimethylbenzene alkylation by 1-decene. ....  | 32 |
| Figure 10. FT-IR spectra of H-PTA/SiO <sub>2</sub> ( <b>1</b> ) and H-PMA/SiO <sub>2</sub> ( <b>4</b> ).....                       | 36 |
| Figure 11. TEM images of sample <b>1</b> .....   | 37 |
| Figure 12. Particle size distribution of <b>1</b> , <b>1-R</b> and <b>14</b> .....   | 38 |
| Figure 13. N <sub>2</sub> adsorption/desorption isotherms and pore size distribution of <b>1</b> .....                             | 39 |
| Figure 14. TGA (red) and DSC (black) curves of sample <b>1</b> . ....  | 40 |
| Figure 15. Comparison of catalytic activity of <b>1</b> , <b>14</b> , pure PTA, HY and HZSM-5 at various<br>temperatures. ....     | 41 |
| Figure 16. Distribution of isomeric alkylbenzenes on samples <b>1</b> , <b>14</b> , PTA and HY. ....                               | 43 |
| Figure 17. GC chromatogram of reaction mixture after alkylation catalyzed by <b>1</b> at 140°C. ....                               | 44 |
| Scheme 1. Alkylation chemistry.....  | 14 |
| Scheme 2. Synthesis of alkylbenzenesulfonates.....   | 15 |
| Scheme 3. Mechanism of benzene alkylation catalyzed by Lewis acid AlCl <sub>3</sub> .....  | 16 |

|   |    |
|---|----|
| Scheme 4. Synthesis of 1,5-benzodiazepine .....   | 18 |
| Scheme 5. Protonation of alkanes over acid zeolites .....                                   | 18 |
| Scheme 6. Sol-gel process reactions .....   | 22 |
| Scheme 7. Condensation of TEOS in sol-gel process.....                                      | 23 |
| Scheme 8. Formation of isomeric alkylbenzenes from 1,3,5-trimethylbenzene and 1-decene. ... | 46 |

## LIST OF ABBREVIATIONS

|                         |  |
|-------------------------|--|
| AAS                     | Atomic absorption spectroscopy                     |
| BAB                     | Branched alkylbenzene                              |
| BET                     | Brunauer-Emmett-Teller theory                      |
| Cs-PTA/SiO <sub>2</sub> | Cesium-exchanged H-PTA/SiO <sub>2</sub>            |
| DDA                     | Dodecylamine                                       |
| DSC                     | Differential scanning calorimetry                  |
| FT-IR                   | Fourier Transform infrared spectroscopy            |
| GC-MS                   | Gas chromatography with mass-spectrometry detector |
| H-PTA/SiO <sub>2</sub>  | Phosphotungstic acid embedded in silica gel        |
| HPA                     | Heteropolyacid                                     |
| HSZ                     | Hierarchically structured zeolite                  |
| LAB                     | Linear alkylbenzene                                |
| LAS                     | Linear alkylbenzene sulfonate                      |
| NMR                     | Nuclear magnetic resonance                         |
| PMA                     | Phosphomolybdic acid                               |
| PTA                     | Phosphotungstic acid                               |
| SDS                     | Sodium dodecylsulfate                              |
| S <sub>N</sub> 2        | Second-order nucleophilic substitution             |
| TEM                     | Transmission electron microscopy                   |
| TEOS                    | Tetraethyl orthosilicate                           |
| TGA                     | Thermogravimetric analysis                         |
| THF                     | Tetrahydrofuran                                    |
| TMS                     | Trimethylstearylammonium chloride                  |

## CHAPTER 1. INTRODUCTION

### *Alkylated Benzenes*

Alkylated benzenes are the major feedstock for manufacturing of large variety of products such as fuels, plastics and detergents. The large-scale commercial production of alkyl benzenesulfonates obtained from alkylaromatic compounds starting in 1940s marked the beginning of the detergent industry based on synthetic surfactants.<sup>1</sup> Earliest industrial process resulted in obtaining branched alkylbenzenes (BABs) that were the initial feedstock for further production of synthetic detergents. However, the branching of alkyl aryls was responsible for decreased biodegradability of the final product. Overtime, BABs got replaced by linear alkylbenzenes (LABs) due to the higher biodegradable nature of the latter.

Nowadays, LAB is a vital intermediate in production of linear alkylbenzene sulfonate (LAS). LAS belongs to a group of skeletal isomers. Their general chemical formula is  $C_6H_5C_xH_{2x+1}$  ( $x = 8-16$ ).

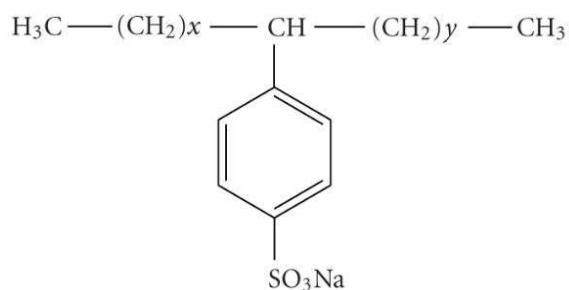
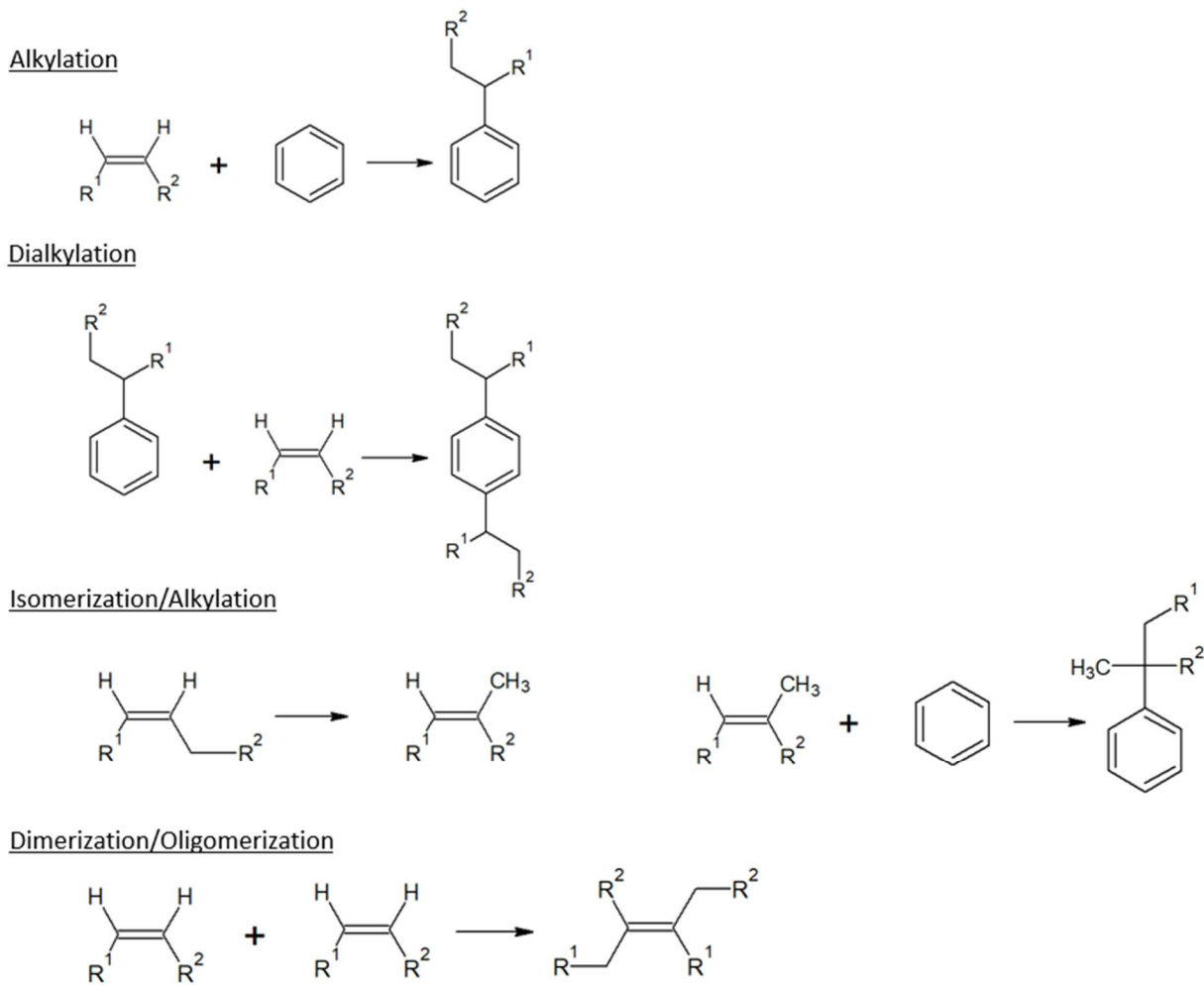


Figure 1. General LAS structure.

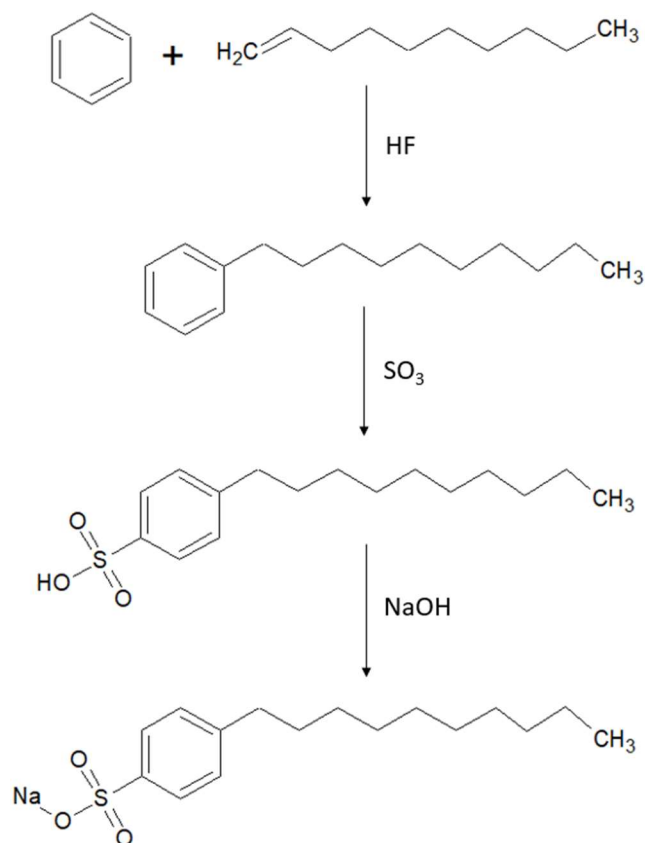
Two main structural parts of the LAS are phenyl group and long alkyl chain. Solubility and biodegradability of a compound is determined by the position of those two parts. LAS is the primary surfactant used in industrial as well as household detergents, thus making LAS the

world's largest volume synthetic surfactant. In recent years, hundreds of millions of kilograms of LAS is being manufactured annually.<sup>3</sup>

Scheme 1 and 2 outline key reactions of commercial route to LAB-LAS production.



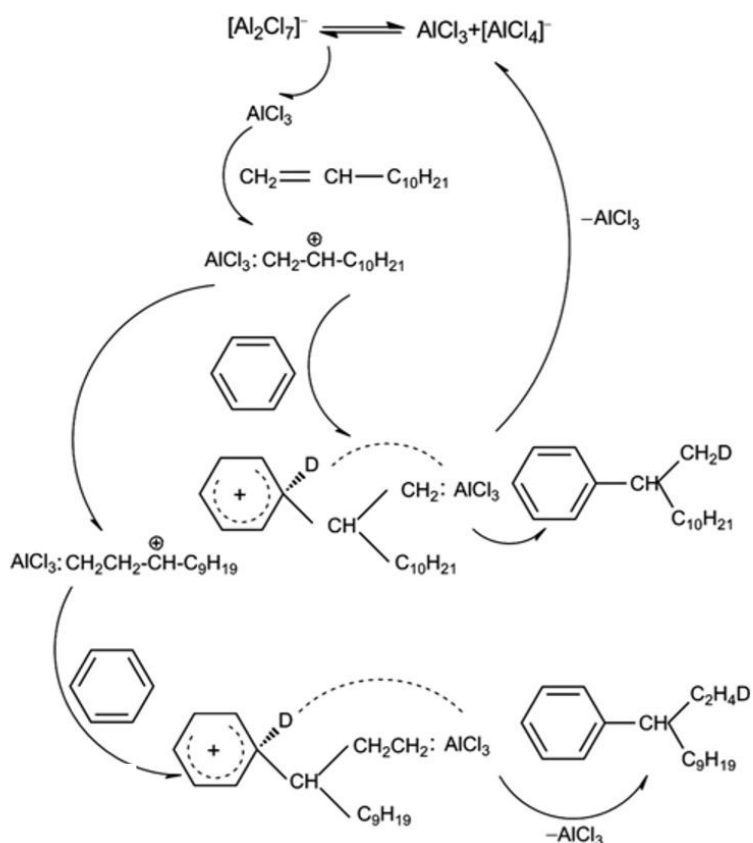
Scheme 1. Alkylation chemistry.<sup>1</sup>



Scheme 2. Synthesis of alkylbenzenesulfonates.<sup>3</sup>

Currently feedstock for LAB-LAS are produced by homogeneous HF- or AlCl<sub>3</sub>-catalyzed liquid phase alkylation of benzene. Two main synthetic routes to production of LAB from olefins and benzene are employed in industrial manufacture. AlCl<sub>3</sub> aids in benzene alkylation with previously chlorinated n-paraffins. Scheme 3 demonstrates the mechanism of AlCl<sub>3</sub>-assisted Friedel-Crafts alkylation.<sup>4</sup> Another way of obtaining LAB requires production of olefins from paraffins by means of monochlorination and dehydrochlorination; obtained olefins are used for benzene alkylation catalyzed by HF. These processes are not environmentally friendly and result in formation of large volume of toxic acidic wastes. In addition, the catalysts used are corrosive to the industrial equipment.





Scheme 3. Mechanism of benzene alkylation catalyzed by Lewis acid  $\text{AlCl}_3$ .

These drawbacks can be eliminated by switch from homogeneous to heterogeneous catalysis. The first solid acid catalyzed technology Delta<sup>TM</sup> was proposed by UOP and is widely utilized for commercial manufacture.<sup>1</sup> “Delta Process” is based on solid bed catalyst system that eliminates the need for hazardous substances like HF.

### *Zeolites*

Over the last decades growing demand for development of environmentally friendly chemical processes caused a notable surge in pursuit of researching and designing reusable solid acid catalysts. Such materials have a potential to replace hazardous liquid acids currently used in multiple processes in chemical industry. Heterogenization of homogeneous catalysts has been suggested as a solution to the problems associated with the use of pure acid catalysts, such as

expensive and rather intricate separation process. Employment of reusable solid acid catalysts simplifies catalytic processing. Among heterogeneous catalysts of benzene alkylation, zeolites are the best studied.<sup>5-8</sup> Zeolites along with heteropolyacids, zirconia, and clays have been utilized as an alternative to corrosive liquid acids.

Zeolites are porous materials with well-defined cage- or channel-like composition

(Figure 2).

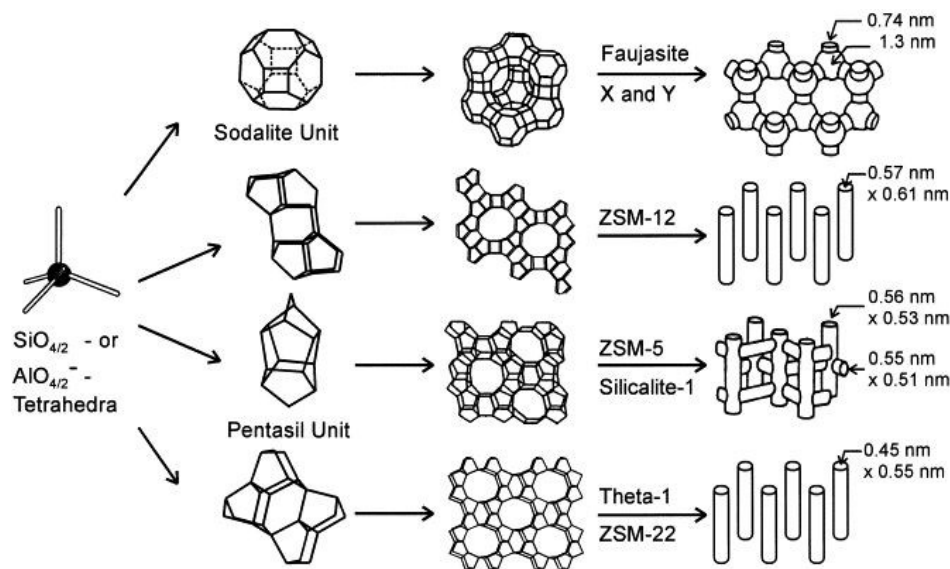
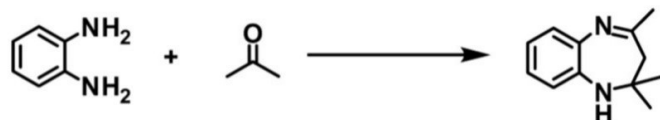


Figure 2. Micropore system and general structure of four zeolites.<sup>9</sup>

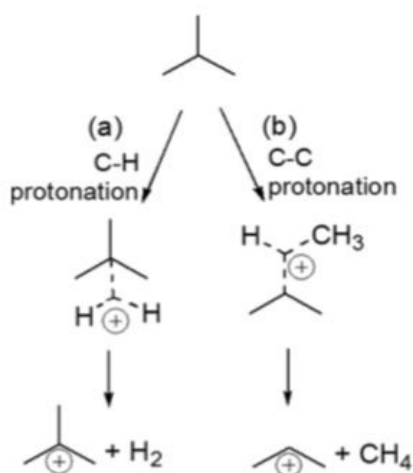
They are crystalline solids containing aluminum, silicon, oxygen in their general network, water and various cations can be found in their micropores. A notable aspect of zeolites structure is the size uniformity of pores and channels. They found many applications in various industrial processes due to highly organized structure and precise pore sizes. Zeolites belong to the family of acidic solid material. This property combined with superior selectivity enables their use in LAB synthesis. Zeolites have been extensively used as powerful catalysts due to their well-

defined pore structure. Jeganathan *et al.*<sup>10</sup> reported efficient synthesis of substituted 1,5-benzodiazepines catalyzed by HY zeolites (Scheme 4).



Scheme 4. Synthesis of 1,5-benzodiazepine.<sup>10</sup>

The constantly growing petrochemical industry created a need for study and development of compounds capable of increasing the production commodities of petrochemical industry, e.g. ethene, propene and butene by the method of catalytic cracking. Zeolites' catalytical properties have been the subject of interest. One of the widely used reactions is zeolite catalyzed  $\alpha$ -protolytic cracking initiated by alkane activation that proceeds through Haag-Dessau mechanism<sup>11</sup>. (Scheme 5).



Scheme 5. Protonation of alkanes over acid zeolites.<sup>12</sup>

Despite reliability of operation offered by steam cracking routinely used in industry, it has several drawbacks such as high reaction temperatures, low propene/ethene ratio, high investment cost, etc.<sup>12</sup> Catalytic cracking method enables production of light olefins and can

overcome mentioned earlier limitations. However, microporous zeolites are limited to catalyzing reactions involving small molecules. Recently, hierarchically structured zeolites (HSZ) have been studied intensively for numerous applications. Besides naturally occurring micropores, HSZs possess mesoporous structures, which resulted in significant improvement of their performance in catalysis.<sup>13</sup> However, zeolites demonstrate high sensitivity to deactivation due to irreversible amorphization.

Other group of solid catalysts is based on clays such as bentonite or montmorillonite.<sup>14-15</sup> Though, the major drawback associated with use of clay for catalytic purposes is their low acidity which results in elevated temperature of alkylation. Ionic liquids<sup>16-18</sup> and aluminum impregnated silica<sup>19</sup> have also been studied as catalysts of benzene alkylation.

The need for developing more versatile and environmentally friendly catalysts led to increased interest in incorporation of catalytically active heteropolyacids (HPAs) into framework of mesoporous materials.

### *Heteropolyacids*

Among the large number of superacidic compounds, heteropolyacids (HPAs) are one of the most interesting. HPAs possess both acidic and redox properties. They belong to a large fundamental class of inorganic compounds. HPAs with well-known Keggin structure have been fully characterized. Keggin heteropolyanions (Fig. 3) have general formula  $\text{XM}_{12}\text{O}_{40}^{n-8}$ , with the central atom X ( $\text{Si}^{4+}$ ,  $\text{P}^{5+}$ , etc.) with an n oxidation state, and M is the metal ion ( $\text{Mo}^{6+}$  or  $\text{W}^{6+}$ ). The counter cations may be  $\text{H}^+$ ,  $\text{H}_3\text{O}^+$  etc. Phosphotungstic acid (PTA) ( $\text{H}_3\text{PW}_{12}\text{O}_{40}$ ) is one of the examples of HPAs. Complete delocalization of electrons over many oxygen atoms is responsible for HPA's characteristic high proton mobility, which results in their superacidity. Therefore,

HPAs are capable of catalyzing various reactions in both homogeneous and heterogeneous environments.<sup>20,21</sup>

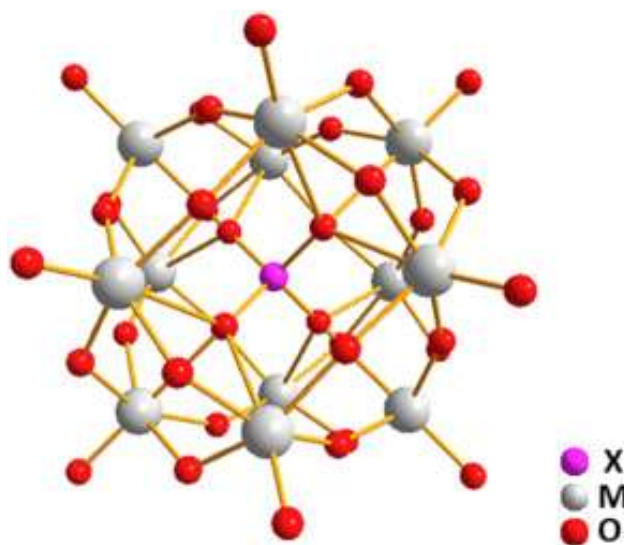


Figure 3. Representation of a generic Keggin structure.<sup>22</sup>

HPAs have become well-known as solid superacids with high catalytic activity in many reactions. However, as it was mentioned earlier, homogeneous catalysis has drawbacks, e.g. difficult and expensive separation of the used catalyst from the reaction mixture and its recycling. Application of pure HPAs in heterogeneous catalysis is limited by their low surface area and solubility in polar solvents. Immobilization of HPAs on solid support results in increase of their surface area. The most common technique for HPA supporting is impregnation of highly porous inert materials such as silica gel, MCM-41 etc. SBA-supported PTA exhibited higher activity and selectivity in alkylation of phenol by *t*-BuOH on supported PTA, the produced *p-t*-butylphenol with high selectivity.<sup>23</sup> SBA-supported PTA exhibited higher activity and selectivity in alkylation of toluene by 1-dodecene than zeolite HY.<sup>24</sup> Aniline reacted with aromatic aldehydes on supported and non-supported PTA. Phenoxy pyrazolyl chalcones synthesis was successfully catalyzed by silica-supported copper-doped phosphotungstic acid

(CuPTA/SiO<sub>2</sub>) obtained by impregnation method.<sup>25</sup> Zhang *et al.* reported excellent catalytic activity demonstrated by PTA immobilized in amine-grafted graphene oxide.<sup>26</sup> Other examples of the use of supported PTA in catalysis are synthesis of ethers,<sup>27</sup> esterification of glycerols,<sup>28</sup> condensation of carbonyl compounds with alcohols,<sup>29</sup> etc.

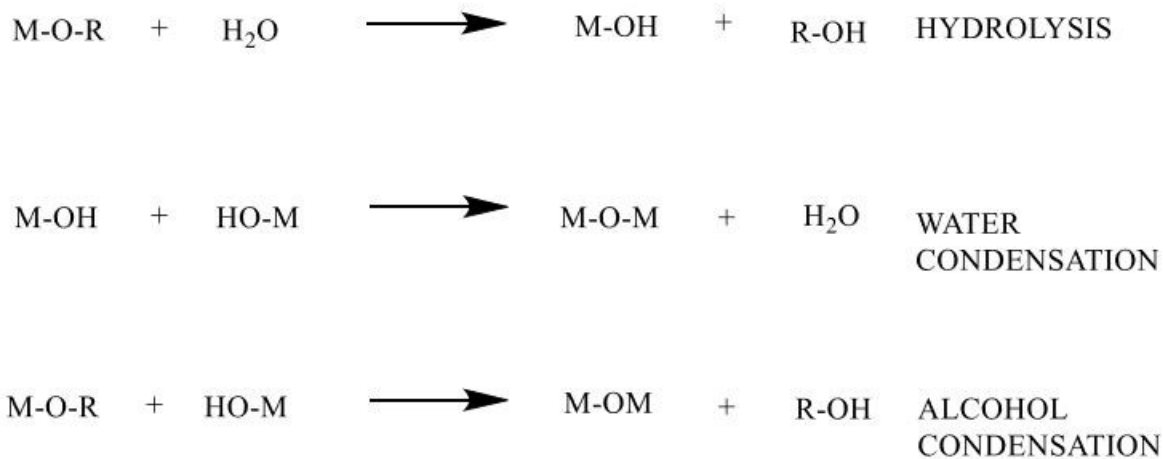
Insoluble cesium salts of PTA also have high catalytic activity, but they have higher surface area than the acidic form.<sup>30</sup> It was explained by growth of porosity at partial ion exchange of protons by cesium cations and, as a result, higher accessibility of acidic sites.

Impregnating HPA entails introduction of an acid to a previously formed solid matrix. Such approach is simple but limited by low loading percentage as well as structural changes leading to attenuated homogeneity of the material.<sup>31</sup> Utilization of this technique results in noticeable leaching of HPA from the surface due to lack of stable bond between introduced acid and the solid support. Considering HPA's high solubility in organic and aqueous solvents, employing impregnation leads to material with low stability and reactivity. Leachability of supported HPAs can be prevented by covalent embedding of an HPA into the matrix of the support. It can be achieved by joint polycondensation of the support's precursor with an HPA using sol-gel technique. Thus, in porous materials obtained with PTA, its molecules were bonded to silica via Si-O-W bridges. In accordance with literature data, the duration of stable work of similar catalysts is much higher than impregnated ones.<sup>32</sup> Catalysts of this type can be easily recycled even from polar solvents.<sup>33</sup> As it was shown earlier, up to 25% of HPAs can be embedded by sol-gel method without significant loss of porosity.<sup>34</sup>

#### *Sol-Gel Method*

The sol-gel method is a popular synthetic approach to obtain fibers, membranes, ceramics, and gels.<sup>35</sup> The sol-gel process (Scheme 6) proceeds in two steps. The first step is a

hydrolysis reaction, which results in formation of silanol group; the second step is a condensation reaction producing siloxane bonds in alcohol/water solutions.<sup>36</sup>

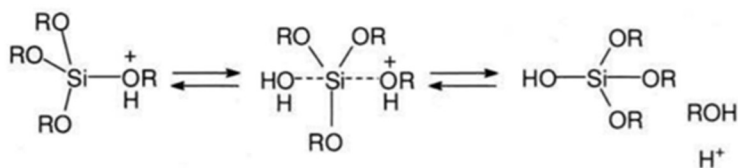


Scheme 6. Sol-gel process reactions.<sup>36</sup>

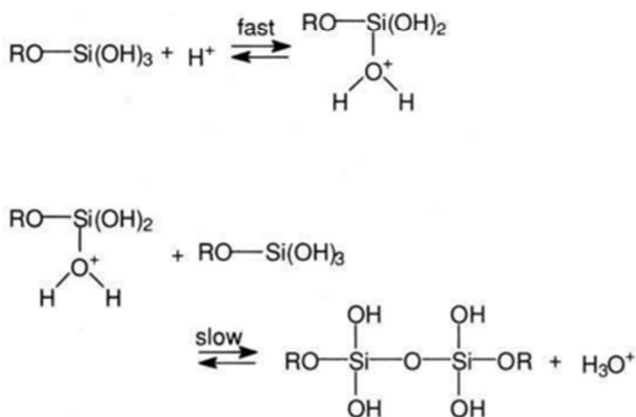
Metal alkoxides can form homogeneous solution in various solvents, they have also demonstrated high reaction affinity toward nucleophiles such as water. There are a few examples of the properties that enable use of metal alkoxides as metal precursors for sol-gel method. Metal alkoxides used in hydrolysis belong to a large group of metalorganic compounds. Silicon tetraethoxide, mostly known as tetraethyl orthosilicate (TEOS) is a commonly used Si precursor (Scheme 7). Hydrolysis and polycondensation are two main reactions leading to gel formation as a result of a stepwise polymerization. Sol-gel processing of TEOS is carried out in polar solvents such as ethanol. The reaction rate can be accelerated in acidic or basic media. However, HPA's low stability in basic environment has determined employment of acidic catalysts.

Polymerization of TEOS is initiated at multiple sites within precursors leading to cross-linked network formed by interconnected Si-O-Si bonds. Acid-catalyzed polymerization proceeds through bimolecular nucleophilic substitution reactions  $S_N2$ .<sup>37</sup>

### Acid-Catalyzed Hydrolysis



### Acid-Catalyzed Condensation



Scheme 7. Condensation of TEOS in sol-gel process.

Sol-gel process reactions are carried out at relatively low temperature; modification of the composition of reaction mixtures allows to control reaction kinetics.<sup>38</sup> Utilization of sol-gel method enables to obtain SiO<sub>2</sub> nanoparticles of few hundred nanometers to several micrometers in size, for example, controlled hydrolysis of TEOS in ethanol resulted in obtaining particles of various sizes.<sup>39</sup>

The parameters of silica nanoparticles can be controlled with organic acids, surfactants, electrolytes etc. Sol-gel condensation around a self-assembled surfactant template allows to make ordered mesoporous materials (Fig. 4).



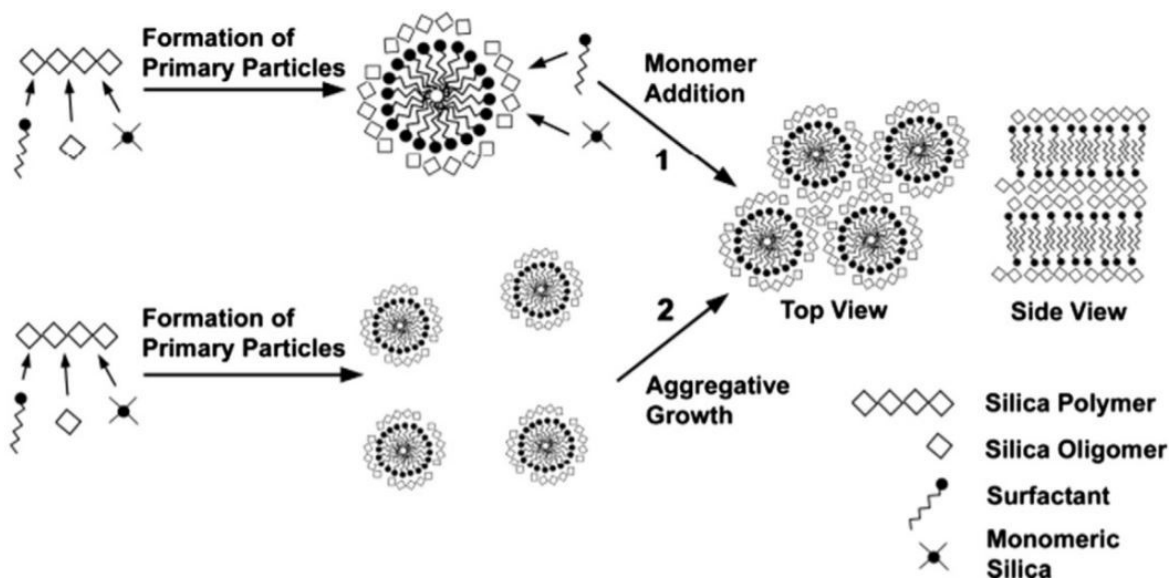


Figure 4. Monomeric silica addition (mechanism 1). Formation of ordered mesoporous structure by aggregation (mechanism 2).<sup>40</sup>

### *Mesoporous Materials*

Mesoporous materials are solids containing pore sizes ranging from 2 to 50 nm. Properties of a mesoporous material and its applications are often defined by porosity. Mesoporous organic-inorganic hybrid materials with various functional groups on the surface have found broad spectrum of application: catalysis, pharmaceutical, electrochemical, adsorption, etc.

Mesoporous materials offer many advantages such as well-defined pore size distribution, corrosion resistance, thermal and chemical stability, controlled pore structure, simple surface modification and large surface area. These properties are responsible for numerous applications of such materials, for example, porous solids are widely used as electrocatalyst support and ultracapacitors.<sup>41</sup> Mesoporous materials can be used as acid catalysts and as supports.<sup>42</sup> Mesoporous hybrid materials are mostly prepared using zeolites and silica as templates. Silica

nanoparticles properties have been actively studied in various applications, e.g. catalysis, pigment synthesis. For example, pharmaceutical industry has utilized advantages offered by a substantial pore volume, well-defined porous structure and high surface area. Mesoporous materials are used for controlled drug delivery; mesoporous silica nanoparticles properties have been intensively studied for application in cancer research, e.g. target drug delivery to the cell of interest.<sup>43</sup> Amorphous silica nanoparticles are utilized in production of electrical and thermal insulators, humidity sensors and various electric substrates. Chemical vapor deposition, plasma synthesis, microemulsion processing, combustion synthesis, sol-gel processing are some of the methods used to synthesize silica nanoparticles.<sup>38</sup>

The synthetic route proposed in this work to obtaining mesoporous catalysts required use of surfactants as pore-forming agents.

### *Surfactants*

Surfactants are chemically unique species with a dual character. Hydrophilic and hydrophobic portions of the chemical structure are responsible for their ability to lower surface tension, thus making them surface active agents. In an aqueous environment, the hydrophilic portion is relatively polar, whereas the hydrophobic portion is relatively non-polar.

Surfactants are classified into three groups: non-ionic, anionic or cationic (Fig. 5-7). For the anionic and cationic species, the hydrophobic portion of a surfactant normally contains a hydrocarbon chain ( $-\text{CH}_2-\text{CH}_2-$ ) and the hydrophilic part includes a variety of chemical functionalities such as a carboxyl ( $-\text{COOH}$ ), amine group ( $-\text{NH}_3$ ), sulphonate ( $-\text{SO}_3$ ), or sulphate ( $-\text{SO}_4$ ) group, etc. Structure of a non-ionic surfactants generally includes various alkoxyates.<sup>44</sup>

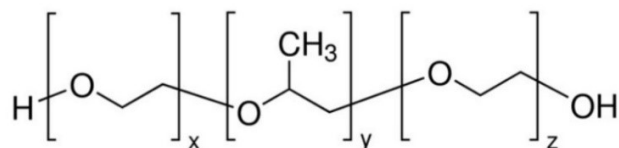


Figure 5. Non-ionic surfactant, PEG-PPG-PEG (Pluronic).

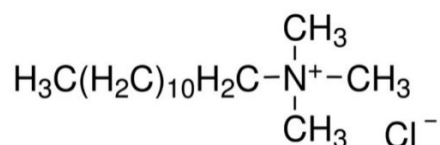


Figure 6. Anionic surfactant, dodecyltrimethylammonium chloride.

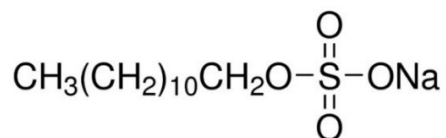


Figure 7. Cationic surfactant, sodium dodecyl sulfate.

### *Research Objectives*

Despite excellent catalytic performance of embedded catalysts, to present time they are not studied as extensively as impregnated catalysts. The objective of this work is the synthesis and study of catalysts with PTA and PMA covalently embedded into the silica matrix.

Mesoporous materials will be obtained applying sol-gel technique using TEOS and HPAs as precursors. Simultaneous co-condensation of TEOS and tungsten- or molybdenum-containing HPA will result in covalent embedding of highly acidic sites into silica matrix. Obtained catalysts will be characterized using TEM (transmission electron microscopy) imaging, solid-state NMR (nuclear magnetic resonance), porosimetry, thermoanalysis, atomic absorption spectroscopy. Their catalytic activity will be tested in liquid phase alkylation of

1,3,5-trimethylbenzene by 1-decene. Composition of reaction mixture will be analyzed using GC-MS (gas chromatography with mass-spectrometry detector).

## CHAPTER 2. EXPERIMENTAL METHODS

### *Reagents Used*

Chemicals used in catalysts synthesis and for alkylation studies are listed in Table 1.

Table 1. Chemicals used

| <b>Reagent Name</b>                      | <b>Chemical Formula</b>  | <b>Supplier</b>                    | <b>Use</b>    |
|--|--|------------------------------------|---------------|
| Tetraethoxysilane (TEOS)                 | $\text{Si}(\text{OC}_2\text{H}_5)_4$   | Acros Organics (Morris Planes, NJ) | Precursor     |
| Phosphomolybdic acid hydrate (PMA)       | $\text{H}_3[\text{P}(\text{Mo}_3\text{O}_{10})_4] \cdot x\text{H}_2\text{O}$   | Acros Organics                     | Precursor     |
| Phosphotungstic acid hydrate (PTA)       | $\text{H}_3[\text{P}(\text{W}_3\text{O}_{10})_4] \cdot x\text{H}_2\text{O}$  | Acros Organics                     | Precursor     |
| Cesium chloride                          | $\text{CsCl}$  | Acros Organics                     | Ion exchanger |
| Dodecylamine (DDA)                       | $\text{C}_{12}\text{H}_{25}\text{NH}_2$  | Acros Organics                     | Surfactant    |
| Sodium dodecyl sulfate (SDS)             | $\text{C}_{12}\text{H}_{25}\text{OSO}_3\text{Na}$  | Acros Organics                     | Surfactant    |
| Trimethylstearyl-ammonium chloride (TMS) | $\text{C}_{18}\text{H}_{37}(\text{CH}_3)_3\text{NCl}$  | TCI (Tokyo, Japan)                 | Surfactant    |
| Pluronic P123                            | $\text{HO}[\text{CH}_2\text{CH}_2\text{O}]_{20}[\text{CH}_2\text{CH}-(\text{CH}_3)\text{O}]_{70}[\text{CH}_2\text{CH}_2\text{O}]_{20}\text{H}$ | Sigma-Aldrich (St. Louis, MO)      | Surfactant    |
| Zeolite HZSM-5 (CBV 5524G)               | $\text{SiO}_2/\text{Al}_2\text{O}_3 = 50$  | Zeolyst Int. (Conshohocken, PA)    | Catalyst      |
| Zeolite HY (CBV 500)                     | $\text{SiO}_2/\text{Al}_2\text{O}_3 = 5.2$   | Zeolyst Int.                       | Catalyst      |
| 1-Decene                                 | $\text{C}_8\text{H}_{17}\text{CH}=\text{CH}_2$   | Acros Organics                     | Reactant      |
| 1,3,5-Trimethylbenzene                   | $\text{C}_6\text{H}_3(\text{CH}_3)_3$  | Sigma-Aldrich                      | Reactant      |

### Synthetic Procedures

Mesoporous materials were synthesized by sol-gel method (Fig. 8). Three solutions were prepared. 2 g of a surfactant was dissolved in 6 mL of ethanol. Precursors TEOS (3.2 g) and HPA (0.4 g) were dissolved in 2 mL of ethanol. Simultaneously, two solutions, one containing TEOS and HPA, the other was HCl solution of various concentrations, were added dropwise to the solution of surfactant while stirring. Pluronic P123 was used for preparation of samples **1-4**. Ionic surfactants were used as templates for preparation of samples **5-7** (DDA), **8-10** (SDS) and TMS was used to obtain **11-13**. Three concentrations of HCl were used in the synthesis: 20% for samples **1, 4, 5, 8, 11**, 2% for **2, 6, 9** and **12** and 0.2% (samples **3, 7, 10, 13**). All samples but **4** (PMA) were prepared with PTA. The reaction mixture was refluxed at 80°C for 24 h. The resulting gel was filtered, washed with deionized water until no longer acidic. After complete removal of acid, materials were rinsed with acetone and air-dried overnight. To ensure removal of the surfactant, samples were calcined at 500°C for 5 h.

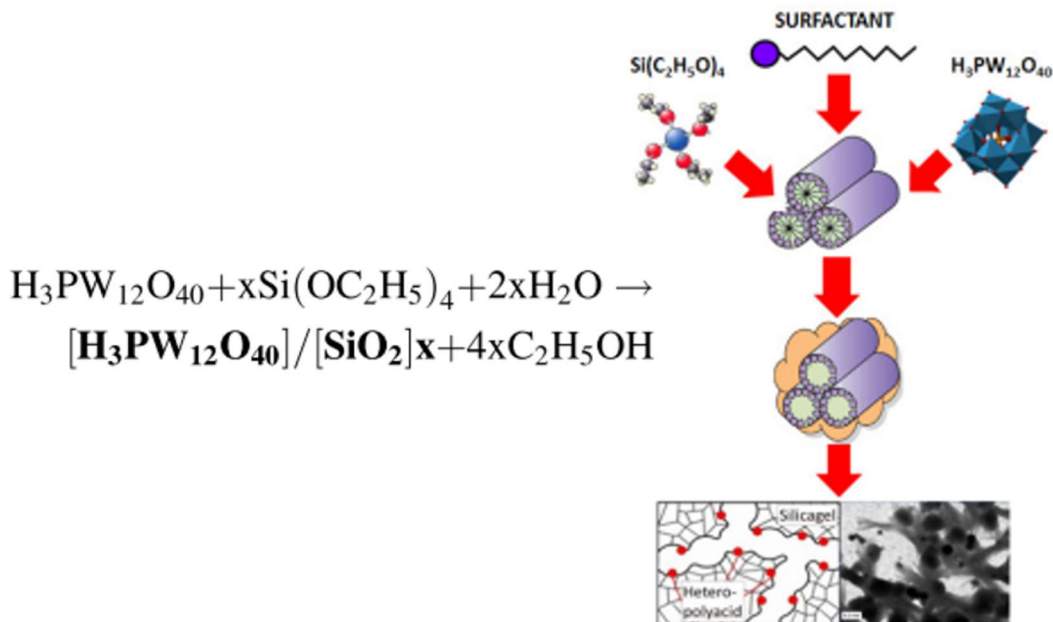


Figure 8. Synthesis of mesoporous materials by sol-gel method.

Sample **14** consisted of Cs-exchanged material which was obtained by mixing 5 g of **1** with 50 mL of 0.12 M CsCl solution. The mixture was stirred for 16 h at room temperature, afterwards exchanged material was washed with deionized water and air-dried overnight.

### *Instrumental Characterization*

#### *Elemental Analysis*

Shimadzu AA-6300 atomic absorption spectrometer (Kioto, Japan) was used for determination of contents of Mo, W and Cs in the samples. The samples were prepared by dissolving synthesized catalysts in 48% HF (VWR International, Radnor, PA). After dissolution samples were neutralized to pH 7 by 25% NH<sub>4</sub>OH. PTA and PMA content were calculated from data obtained using AAS.

#### *Surface acidity*

Surface acidity of synthesized materials was determined by reverse titration. Considering HPAs instability in aqueous environment at elevated pH, neutralization of acidic sites was performed in anhydrous THF. Prior to titration, samples were dehydrated at 150°C for 3 h. 0.1 g of each sample was placed in 6 mL of 0.01 M pyridine in THF solution. The mixture was left to equilibrate overnight at room temperature. Afterwards, 4 mL of equilibrated solution was diluted with 100 mL of deionized water and titrated with 0.01 M HCl until pH=3. Blank solution was prepared by diluting 4 mL of 0.01 M pyridine/THF solution with 100 mL of DI water.<sup>45</sup> pH data was recorded on an Orion 350 pH meter (Thermo Scientific, Pittsburg, PA).

### *Fourier-Transform Infrared (FT-IR) Spectroscopy*

FT-IR spectra were recorded in KBr pellets on a Genesis II spectrometer (Mattson, PA). Analysis of FT-IR spectra of all samples revealed presence of characteristic bands of silica gel at 805 ( $\beta_{\text{Si-O-Si}}$ ), 1088 ( $\nu_{\text{Si-O-Si}}$ ), 1637 ( $\text{H}_2\text{O}$ ), and 3445 ( $\nu_{\text{SOH}}$ )  $\text{cm}^{-1}$ .

### *Transmission Electron Microscopy (TEM)*

TEM imaging was performed on a JEOL 1230 electron microscope (Tokyo, Japan) at 80 kV. Prior to imaging, materials were dispersed in a 50% ethanol solution using a W-385 sonicator (Heat systems Ultrasonic, Newtown, CT) for 2 min.

### *Porosity*

Quantachrome Nova 2200e porosimeter (Boynton Beach, FL) was used to obtain porous characteristics. Before measurements, the samples were degassed in vacuum at 500°C for 2 h.  $\text{N}_2$  was an adsorbate for obtaining adsorption/desorption isotherms. Adsorption branch of isotherms in the range  $P/P_0=0.2-0.4$  were used to calculate the Brunauer-Emmett-Teller (BET) surface area. Particle sizes were analyzed by dynamic light scattering on a Zetasizer Nano ZS90 (Malvern, UK). Prior to measurements, samples were sonicated in DI water for 5 min.

### *Thermoanalysis*

Robertson Microlit Lab (Ledgewood, NJ) conducted differential scanning calorimetry (DSC) and thermogravimetric (TGA) analysis. DSC analysis was performed on a Pyris Diamond differential scanning calorimeter (Perkin Elmer, Waltham, MS). TGA analysis was performed on a Perkin Elmer TGA 7 analyzer. Temperature was increased at rate of 10°C/min.



## Alkylation of 1,3,5-Trimethylbenzene by 1-Decene

### Procedure

Prior to alkylation, catalyst was dehydrated in vacuum at 400°C for 2 h. 50 mg of dehydrated sample was mixed with 5 mL of 1,3,5-trimethylbenzene and 1-decene (4:1 molar ratio) solution. The reaction mixture was kept in hot oil bath for 2 h under stirring at constant temperature (Fig. 9). Reaction proceeded at various temperatures: 100, 110, 120, 130, 140, 150 and 160°C.

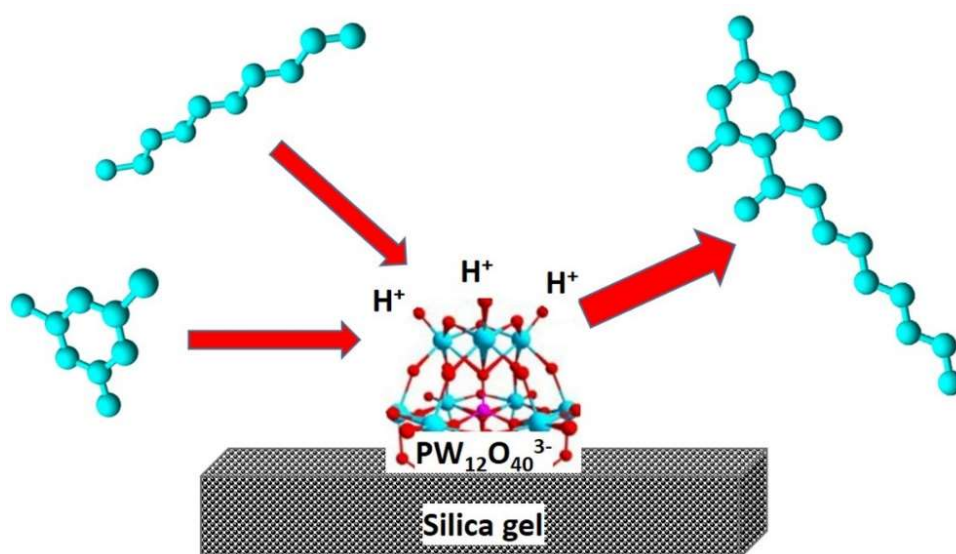


Figure 9. 1,3,5-Trimethylbenzene alkylation by 1-decene.

### GC-MS analysis

After completion, liquid was decanted from solid catalyst and reaction mixture composition was analyzed by gas chromatography on a Shimadzu GCMS-QP2010 Plus (Kioto, Japan). Rtx-5MS capillary column (30 m x 0.25 mm) at 50°C was used for components separation. The column flow rate was 21.9 mL/min with He as a carrier gas. Retention times of reagents were (min): 1,3,5-trimethylbenzene, 5.48; 1-decene, 5.70. Formed isomeric

alkylbenzenes were detected at following retention times (min):

5-(2,4,6-trimethylphenyl)decane, 11.36; 4-(2,4,6-trimethylphenyl)decane, 11.44;

3-(2,4,6-trimethylphenyl)decane, 11.56; 2-(2,4,6-trimethylphenyl)decane, 11.83.

## CHAPTER 3. RESULTS

### *Synthesis and Chemical Composition*

#### *Synthesis*

Gelation of the reaction mixture for all the samples was observed either upon combining reagent solutions prior to refluxing or shortly after the start of reflux. Yields of the synthesized products corresponded to 58.1-79.3% conversion of precursors TEOS and HPA to the modified mesoporous material (Table 2).

#### *Content of Immobilized Heteropolyacid*

Tungsten content in the obtained catalysts was ranging from 23 to 151 mg/g, which indicated 0.010-0,069 mmol/g of immobilized HPA. Density of PTA anions on the surface of the material was determined to be 0.071 molecules of PTA per nm<sup>2</sup>; calculation was done taking in account BET surface area of sample **1**. Subjecting the samples to high temperatures during calcination did not affect HPA content due to stability of Keggin's structure, which was previously confirmed.<sup>34</sup> Cs-exchanged material contained 0.059 mmol/g PTA and 0.15 mmol/g of Cs (2.54 molar ratio Cs/PTA).<sup>45</sup>

#### *Surface Acidity*

Concentration of acidic sites on catalysts surface determined from pyridine absorption (Table 2) was in the range 0.165-0.325 mmol/g, which indicated proton surface density of 0.11-0.33 per nm<sup>2</sup>. Materials obtained with Pluronic P123 (**1-3**) were determined to be the most acidic.

Table 2. Characteristics of the catalysts

| <b>Sample</b> | <b>Yield,<br/>%</b> | <b>BET surface<br/>area, m<sup>2</sup>/g</b> | <b>Mean particle<br/>size, nm</b> | <b>PDI</b> | <b>Contents of<br/>HPA, mmol/g</b> | <b>Acidity,<br/>mmol/g</b> |
|---------------|---------------------|--|-----------------------------------|------------|------------------------------------|----------------------------|
| <b>1</b>      | 66.0                | 585.4  | 332                               | 1.0        | 0.07                               | 0.33                       |
| <b>1-R</b>    | -                   | 498.9  | 642                               | 0.6        | 0.07                               | 0.32                       |
| <b>2</b>      | 58.1                | 645.9  | 314                               | 0.8        | 0.04                               | 0.20                       |
| <b>3</b>      | 42.3                | 762.5  | 294                               | 0.7        | 0.04                               | 0.19                       |
| <b>4</b>      | 71.1                | 591.1  | 144                               | 1.0        | 0.02                               | 0.18                       |
| <b>5</b>      | 72.4                | 679.8  | 302                               | 0.4        | 0.02                               | 0.18                       |
| <b>6</b>      | 72.2                | 854.8  | 320                               | 0.7        | 0.03                               | 0.18                       |
| <b>7</b>      | 73.3                | 520.1  | 362                               | 1.0        | 0.04                               | 0.17                       |
| <b>8</b>      | 65.1                | 631.8  | 316                               | 0.6        | 0.01                               | 0.18                       |
| <b>9</b>      | 66.4                | 380.0  | 308                               | 0.8        | 0.03                               | 0.18                       |
| <b>10</b>     | 65.1                | 458.8  | 334                               | 0.8        | 0.03                               | 0.18                       |
| <b>11</b>     | 79.3                | 1000.6                                       | 272                               | 1.0        | 0.04                               | 0.18                       |
| <b>12</b>     | 66.7                | 283.9  | 307                               | 1.0        | 0.01                               | 0.18                       |
| <b>13</b>     | 59.7                | 557.0  | 266                               | 0.8        | 0.02                               | 0.18                       |
| <b>14</b>     | -                   | 362.7  | 615                               | 0.8        | 0.03                               | 0.06                       |
| <b>PTA</b>    | -                   | 0.3  | -                                 | -          | 0.35                               | 1.57                       |
| <b>HY</b>     | -                   | 567.1  | 778                               | 0.7        | -                                  | 0.21                       |
| <b>HZSM-5</b> | -                   | 452.3  | 478                               | 0.2        | -                                  | 0.18                       |

Concentration of acidic sites in **2** (0.20 mmol/g) and **3** (0.19 mmol/g) was comparable to zeolite HY (0.21 mmol/g). Sample **1** (0.33 mmol/g) contained 7.6 protons per Keggin structure and was the most acidic. Samples obtained with ionic surfactants had lower acidity compared to HY.

### *Structural Characteristics*

#### *Fourier-Transform Infrared (FT-IR) Spectroscopy*

Fig. 10 illustrates FT-IR spectra of samples **1** and **4**. Formation of silica matrix is indicated by the presence of the following bands typical for silica gel: 805, 1088 and 1654  $\text{cm}^{-1}$ . Incorporation of PTA into the silica matrix validated by the presence of a broad band at 963  $\text{cm}^{-1}$  typical for O-W-O stretches.

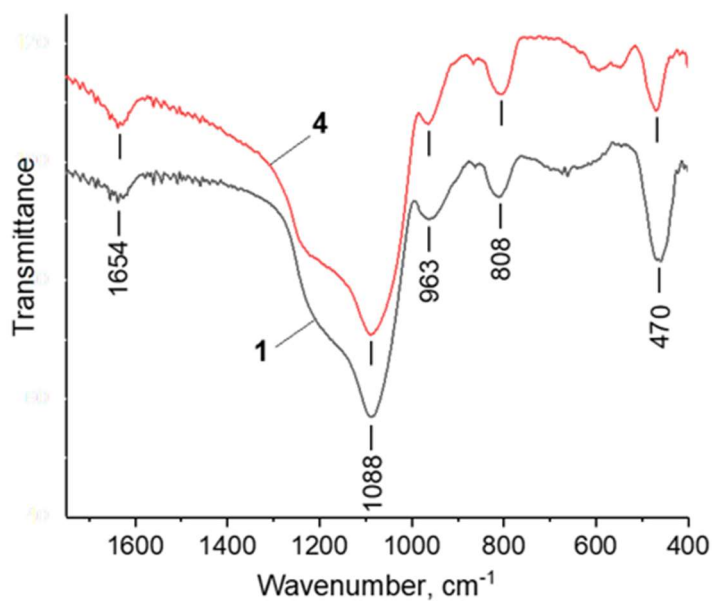


Figure 10. FT-IR spectra of H-PTA/SiO<sub>2</sub> (**1**) and H-PMA/SiO<sub>2</sub> (**4**).

### *Transmission Electron Microscopy (TEM)*

Disordered mesoporous structure of the synthesized materials was revealed by TEM images. TEM analysis of sample **1** indicated presence of particles ranging from 100 nm to 1  $\mu\text{m}$  with pores of 3-6 nm in size (Fig. 11). Clusters of immobilized HPAs appeared as small black spots. Considering the size of a single Keggin's anion determined to be 1.1 nm and the phase contrast properties of W in the incident electron beam<sup>27</sup>, those dark spherical nanoparticles 10-15 nm in diameter represented agglomerations of PTA. All samples had a very similar structure.

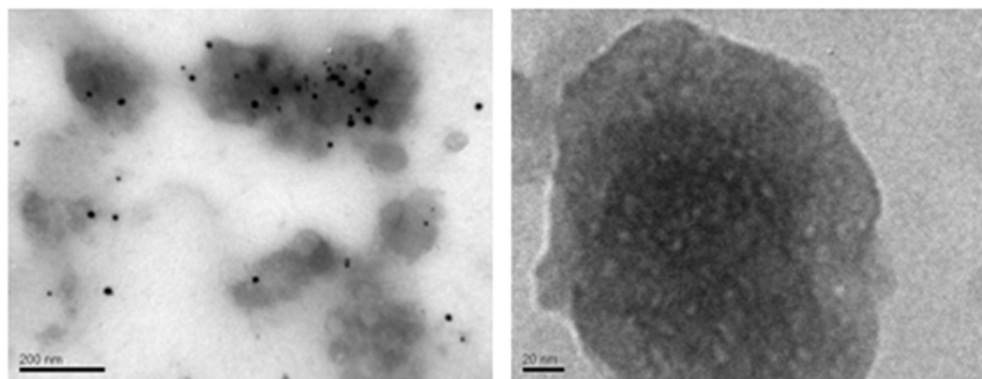


Figure 11. TEM images of sample **1**.

### *Particle Size*

Particle size analysis based on DLS measurements indicated relatively narrow range of sizes (266-362 nm) of materials containing immobilized PTA (Table 1). Those samples also had high PDI and did not indicate agglomeration. Fig. 12 illustrates comparison of particle size distribution of 3 materials: sample **1** (H-PTA/SiO<sub>2</sub>), **1-R** (recycled 1) and **14** (Cs-exchanged material). **1** had the narrowest particle size distribution with the mean value of 332 nm, however, exchange on Cs resulted in noticeable increase in agglomeration of the material. H-PMA/SiO<sub>2</sub> formed particles of smaller size compared to materials obtained with PTA.

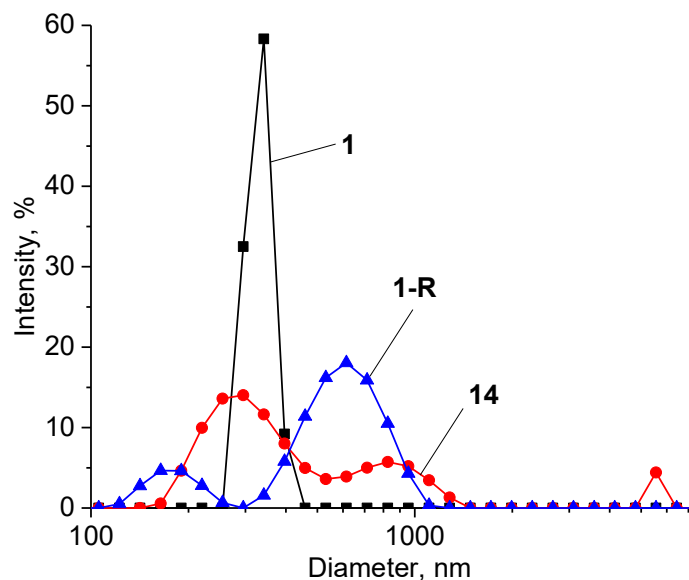


Figure 12. Particle size distribution of **1**, **1-R** and **14**.

### *Porosity*

All synthesized catalysts were mostly mesoporous but with significant amount of micropores in their structure. Obtained N<sub>2</sub> adsorption/desorption isotherms of **1** (Fig. 13) belong to the type IV with H2 type of hysteresis loop. Thus, it was determined that samples obtained with Pluronic P123 as a template had pores of cylindrical shape with necks. Presence of necks in the mesoporous structure was concluded upon examination of the shape of desorption branch.

Varying HCl acid concentration during the synthesis affected the BET surface area of the final product. The following trends were noted: for materials obtained with Pluronic P123, reduction of the acidity of the reaction mixture resulted in an increase of BET surface area, while for most of the samples obtained with ionic surfactants lower acidity led to decrease of BET surface area (Table 1). Sample **1** had the following porosity characteristics: total pore volume of 0.6 cm<sup>3</sup>/g with mean pore diameter of 1.85 nm, micropore volume was 0.05 cm<sup>3</sup>/g with mean

diameter of 0.45 nm. Material **14** obtained with Cs exchange (Cs-PTA/SiO<sub>2</sub>) had smaller BET surface area and overall decrease of the total pore volume.

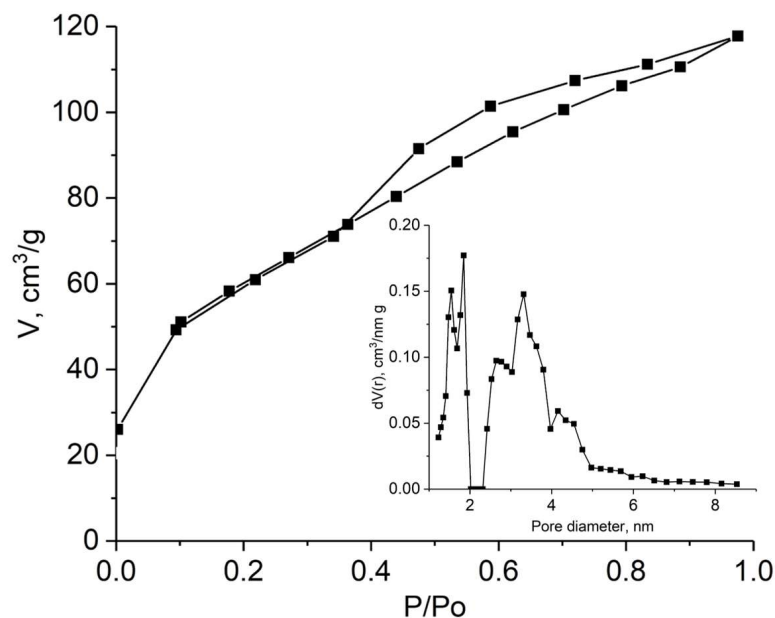


Figure 13. N<sub>2</sub> adsorption/desorption isotherms and pore size distribution of **1**.

### *Thermoanalysis*

Thermoanalysis indicated much higher thermal stability of the synthesized material **1** compared to zeolites, which was pivotal to the possibility of catalyst's regeneration and recycling.

Fig. 14 illustrates obtained TGA and DSC graphs. The TGA curve (in red) of **1** revealed an abrupt weight loss with temperature increase to 100°C. This 8% decrease in mass can be explained by the evaporation of the water molecules physically adsorbed onto the surface. During following increase of the temperature from 100 to 700°C, sample lost only 4% of its total weight. Such gradual decrease in mass was attributed to the dehydration of the sample. In that temperature range simultaneous dehydration of both silica and PTA took place.



DSC curve (in black) allowed detection of phase change in sample **1** indicated by endothermic peak at 187°C with  $\Delta H=572$  J/g. Marosi *et al.* described such event for pure PTA<sup>47</sup>. This endothermic process was explained by changes in lattice dimensions (from 12.17 to 11.78 Å) with retention of the cubic structure.

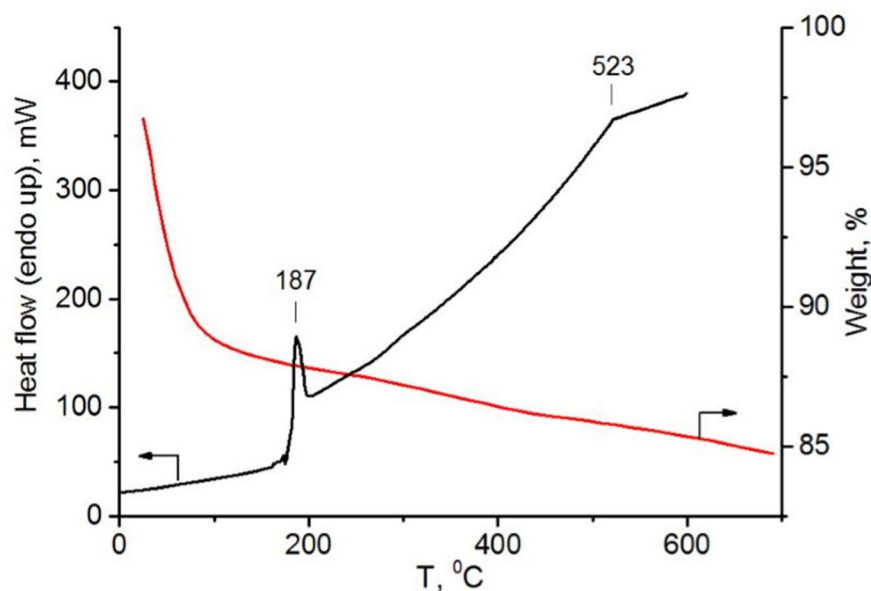


Figure 14. TGA (red) and DSC (black) curves of sample **1**.

### *Catalytic Activity*

Composition of reaction mixture after alkylation was examined using GC-MS. The analysis revealed presence of formed isomeric alkylbenzenes, isomeric decenes and remaining 1,3,5-trimethylbenzene.

### *Effect of Temperature on Catalytic Activity*

Sample **1** demonstrated the highest catalytic activity in conversion of alkene to alkylbenzenes, exceeding zeolite HY. Comparison of catalytic activity of 5 different materials is illustrated in Fig. 15.

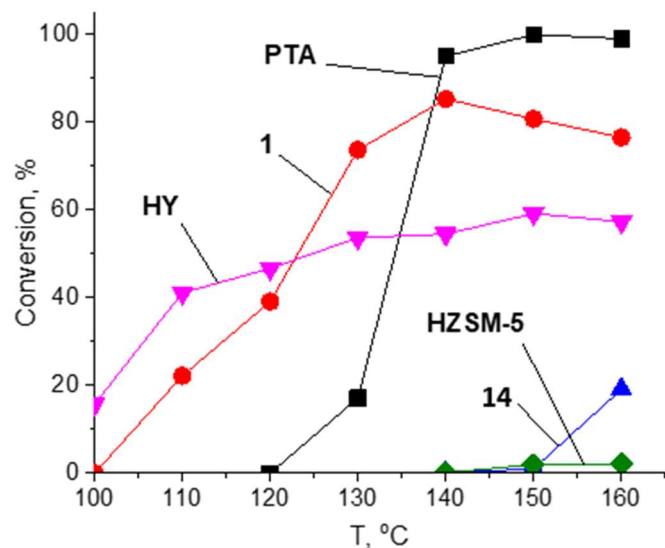


Figure 15. Comparison of catalytic activity of **1**, **14**, pure PTA, HY and HZSM-5 at various temperatures.

Conversion of the reactants to the product catalyzed by sample **1** started above 100°C followed by a gradual increase of activity with highest conversion rate at 140°C.

#### *Effect of HCl Concentration on Catalytic Activity*

Based on conversion data it was concluded that initial acidity of the reaction mixture during sol-gel process had a crucial effect on catalytic performance. Catalyst **3** obtained with 0.2% HCl resulted in 2.5% yield of alkylbenzenes comparing to catalyst **1** (90.3% yield) obtained with 20% HCl (Table 3).

However, using ionic surfactants as templates did not reveal such a distinct trend. Catalyst obtained with SDS (**8-10**) and 0.2% HCl (**10**) was the most effective, while catalysts synthesized in presence of DDA (**5-7**) and TMS (**11-13**) and 2% HCl (**6** and **12** respectively) demonstrated the highest activity. Overall, materials obtained with ionic surfactants showed low catalytic activity with conversion below 11%.

Table 3. Catalytic activity

| Sample        | Reagents                | Yield of alkyl-benzenes (140 °C), % |
|---------------|-------------------------|-------------------------------------|
| <b>1</b>      | PTA/Pluronic/20%HCl     | 90.3                                |
| <b>2</b>      | PTA/Pluronic/2%HCl      | 25.6                                |
| <b>3</b>      | PTA/Pluronic/0.2%HCl    | 2.5                                 |
| <b>4</b>      | PMA/Pluronic/20%HCl     | 0.1                                 |
| <b>5</b>      | PTA/DDA/20%HCl          | 3.7                                 |
| <b>6</b>      | PTA/DDA/2%HCl           | 11.0                                |
| <b>7</b>      | PTA/DDA/0.2%HCl         | 1.2                                 |
| <b>8</b>      | PTA/SDS/20%HCl          | 0.1                                 |
| <b>9</b>      | PTA/SDS/2%HCl           | 3.7                                 |
| <b>10</b>     | PTA/SDS/0.2%HCl         | 4.9                                 |
| <b>11</b>     | PTA/TMS/20%HCl          | 2.5                                 |
| <b>12</b>     | PTA/TMS/2%HCl           | 4.9                                 |
| <b>13</b>     | PTA/TMS/0.2%HCl         | 0.1                                 |
| <b>14</b>     | Cs-PTA/SiO <sub>2</sub> | 0.1                                 |
| <b>PTA</b>    | -                       | 95.0                                |
| <b>HY</b>     | -                       | 54.5                                |
| <b>HZSM-5</b> | -                       | 0.1                                 |

Despite excellent catalytic activity of **1**, Cs-exchanged material **14** overall demonstrated very poor conversion of reactants to alkylated products with a slight increase at 160°C.

### Isomeric Composition of Alkylated 1,3,5-Trimethylbenzenes

All alkylation reactions produced a mixture of isomeric alkylated 1,3,5-trimethylbenzenes. Analysis of compositions of obtained products showed that catalyst **1** had higher selectivity in comparison to homogeneous PTA, 49.5% vs 42.2% (Figure 16). Cs-PTA/SiO<sub>2</sub> selectivity was reduced. HY demonstrated superior selectivity that was due to well-defined structural system characteristic for zeolites.

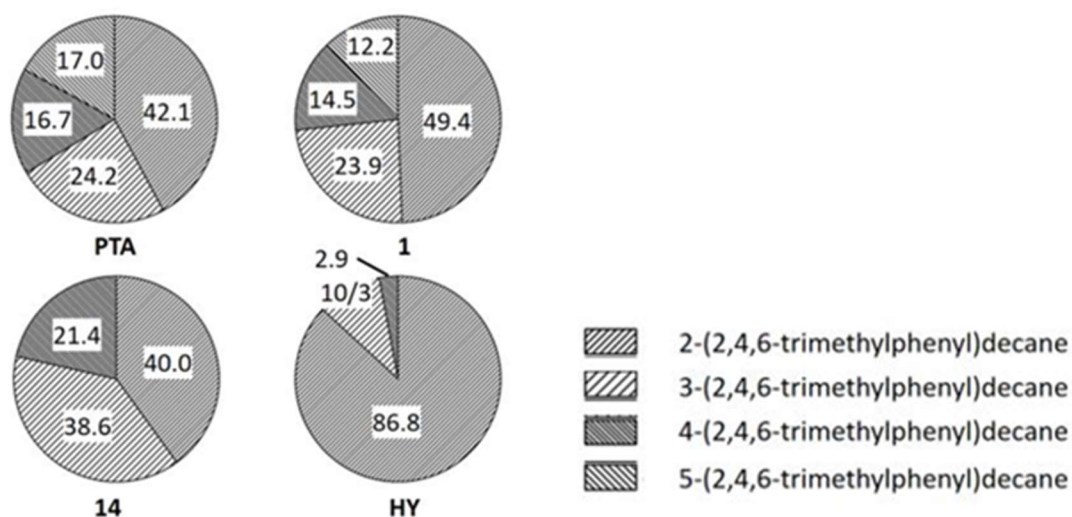


Figure 16. Distribution of isomeric alkylbenzenes on samples **1**, **14**, PTA and HY.

GC-MS analysis revealed isomerization of 1-decene into 2-, 3-, 4-, 5-decenes and distribution of formed isomeric alkylated 1,3,5-trimethylbenzenes (Fig. 17).

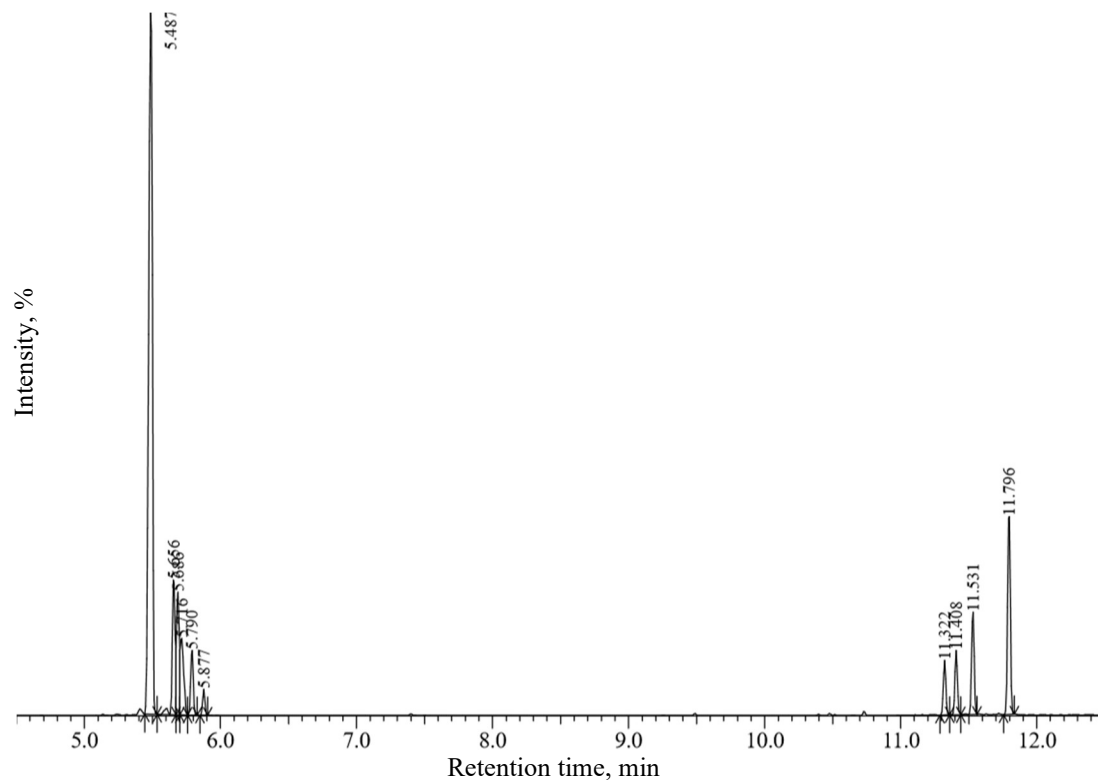


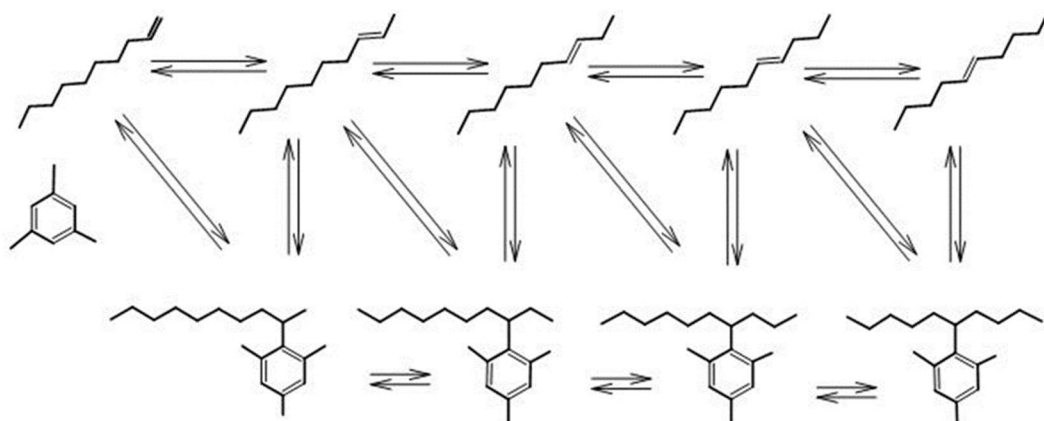
Figure 17. GC chromatogram of reaction mixture after alkylation catalyzed by **1** at 140°C.

It was previously determined that at thermodynamic equilibrium the decene mixture contains 1% of 1-decene.<sup>48</sup> However, analysis of reaction mixture formed on catalyst **1** revealed the following isomeric distribution: 1-decene was dominant isomer at 40.9%, in terms of alkylated product, selectivity on 2-(2,4,6-trimethylphenyl)decane was 49.4%. Pure PTA demonstrated increased alkylating and isomerizing capability. Isomers distribution was determined from GC-MS spectrograms based on retention times and fragmentation patterns (Table 4).

Table 4. Isomeric alkylbenzenes formed on catalyst **1** at 140°C

| Isomeric alkylbenzene            | Retention time (min) | Structure and MS spectra |
|----------------------------------|----------------------|--------------------------|
| 2-(2,4,6-trimethylphenyl)-decane | 11.83                |                          |
| 3-(2,4,6-trimethylphenyl)-decane | 11.56                |                          |
| 4-(2,4,6-trimethylphenyl)-decane | 11.44                |                          |
| 5-(2,4,6-trimethylphenyl)-decane | 11.36                |                          |

Scheme 8 shows two possible ways of isomeric products formation: alkylation of 1,3,5-trimethylbenzene by decene isomers or isomerization of already formed 2-(2,4,6-trimethylphenyl)decane.



Scheme 8. Formation of isomeric alkylbenzenes from 1,3,5-trimethylbenzene and 1-decene.

#### *Recycling of the Catalyst*

Sample **1** was subjected to subsequent round of alkylation immediately following the initial run. Analysis of the catalyst after recycling revealed minimal decrease of acidity and BET surface area as well as unchanged PTA contents, though loss of activity was observed (Table 5).

Table 5. Characteristics of **1** after initial (**1**) and subsequent (**1-R**) round of alkylation

| <b>Sample</b> | <b>BET surface area, m<sup>2</sup>/g</b> | <b>Mean particle size, nm</b> | <b>PDI</b> | <b>Contents of HPA, mmol/g</b> | <b>Acidity, mmol/g</b> | <b>Yield of alkylbenzenes (140°C), %</b> |
|---------------|--|-------------------------------|------------|--------------------------------|------------------------|--|
| <b>1</b>      | 585.4                                    | 32                            | 1.0        | 0.07                           | 0.33                   | 90.3                                     |
| <b>1-R</b>    | 498.9                                    | 642                           | 0.6        | 0.07                           | 0.32                   | 51.6                                     |

## CHAPTER 4. DISCUSSION

### *Characteristics of the Catalysts*

Use of HPA and TEOS as precursors in sol-gel processing resulted in obtaining silica gel with covalently embedded PTA units into the materials structure, which was determined by previously analyzed solid state  $^{29}\text{Si}$  NMR spectroscopy.<sup>45</sup> Initially, covalent immobilization of HPA was proposed to overcome leachability issue, validity of that proposition was evident from AAS data showing unchanged contents of tungsten after catalyst's recycling.

Comparison of two HPAs revealed that amount of PTA incorporated into silica matrix was higher than PMA (**4**) at the same synthesis conditions. Varying contents of embedded PTA (0.02-0.07 mmol/g) in obtained samples was influenced by acidity and type of surfactant. Samples **1** and **2** had the highest amounts of PTA. Upon examining the chemical composition of the products, it was clear that a fraction of the starting amount of HPA got incorporated into the synthesized materials. Initial molar ratio HPA/Si of 0.01 decreased to 0.0043 (catalyst **1**) after the reaction was complete. Yields of obtained mesoporous materials in the range of 58.1-79.3% could be explained by incomplete embedding of PTA.

Acidity studies showed that entrapped HPAs demonstrated high absorption ability on pyridine. Each HPA anion could absorb from 2.7 to 9.6 molecules of pyridine, which exceeded amount of present  $\text{H}^+$  cations. Such behavior of superacids has been observed before; it was established that the number of absorbed cations per one HPA anion can surpass 17.<sup>49</sup>

Study of the number of acidic sites on the surface of obtained materials led to the conclusion that use of non-ionic Pluronic P123 as a template resulted in formation of the most acidic catalyst. Lower acidity of other materials could be due to PTA's interaction with ionic



surfactants. As it was mentioned earlier, PTA is prone to decomposition at elevated pH.<sup>50</sup> Presence of a basic surfactant DDA might have increased instability and partial decomposition. Ion exchange might be responsible for reduced acidity of the samples obtained with TMS and SDS. TMS,  $[\text{C}_{18}\text{H}_{37}(\text{CH}_3)_3\text{N}^+]\text{Cl}^-$ , could neutralize PTA's active sites. Interaction with SDS led to conversion of acidic  $\text{H}^+\text{PTA}$  sites to neutralized  $\text{Na}^+\text{PTA}$  sites, thus lowering overall number of catalytically active sites. Non-Ionic Pluronic P123 was unreactive towards PTA during synthesis.

Samples obtained with Pluronic P123 revealed the following trend concerning varying HCl concentration during synthesis: decrease of acid concentration led to reduced PTA contents, particle size and overall yields, though BET surface area increased. In case of synthesis using ionic surfactants, effect of HCl concentration on the outcome of the reaction was unclear. This could be attributed to the changes in reaction media from acidic to slightly basic (sample **7** obtained with DDA).

Sample **14** obtained by Cs-exchange had lower BET surface area and decreased surface acidity in comparison to **1**. These changes in material characteristics could be due to almost complete proton replacement by larger size of  $\text{Cs}^+$  cations. Even though non-supported  $\text{Cs}_{2.5}\text{H}_{0.5}\text{PW}_{12}\text{O}_{40}$  was determined to have higher acidity as compared to  $\text{H}_3\text{PW}_{12}\text{O}_{40}$ <sup>51</sup> and proved to be effective catalysts in alkylation of aromatic compounds, possible pore blocking by large  $\text{Cs}^+$  prevented reagents from accessing catalytically active acidic sites, thus resulting in poor catalytic performance of sample **14**. It was shown (Fig. 12) that material **14** tended to agglomerate, unlike mentioned earlier non-supported  $\text{Cs}_{2.5}\text{H}_{0.5}\text{PW}_{12}\text{O}_{40}$ . Such behavior could be explained by reduction of the radius of protective layer of the particles caused by the ionic strength of the solution of CsCl used to obtain immobilized Cs-PTA/SiO<sub>2</sub>. The effect of the

solution led to increase of van der Waals radius over the particles radius, thus resulting in observed agglomeration.<sup>52</sup>

### *Catalytic Properties*

Testing of catalytic properties of synthesized materials revealed that most of the samples showed alkylating activity (Table 3). Catalysts **1** and **2** demonstrated the highest conversion of alkene to alkylated product. The catalytic activity of these materials resulted from high surface acidity. Number of active acidic sites on other samples was notably lower, thus decreasing catalytic performance. In case of use of ionic surfactants, the strongest acidic sites could have reacted with surfactant, which led to their deactivation.

Catalysts active in alkylation also demonstrated isomerizing ability. It has been previously established that phenyldecenes isomerize at insignificant rates,<sup>53</sup> which led to the conclusion that presence of catalyst was responsible for the final isomeric composition of the reaction mixture. Analysis of the reaction mixture after alkylation on catalyst **1** revealed that the rate of alkylation was higher as compared to the rate of decene isomerization. Unreacted alkene was determined to have the following composition: 1-decene contributed the most to the mixture at 35.6%, while 5-decene was present in trace amount at 5.2%, the remaining isomers 2-,3- and 4-decene were 26.0, 19.3 and 13.9%.

Cs-exchanged material demonstrated rather poor catalytic activity. It should be noted that unsupported Cs-PTA has been reported to be highly effective as a catalyst.<sup>54-56</sup> Okuhara et al.<sup>30</sup> explained such a high catalytic activity demonstrated by non-supported Cs-PTA by easier access to the active sites, which in turn was accomplished by the increase in BET surface area of the

particles after Cs-exchange. However, in our case such structural changes were negligible due to the covalent incorporation of the Keggin elements.

Catalytic performance of synthesized catalyst **1** was compared to the activity of zeolites HY and H-ZMS-5. H-PTA/SiO<sub>2</sub> proved to be more effective at higher temperatures while HY demonstrated better catalytic activity below 110°C (Fig. 15). Despite strong acidic sites H-ZSM-5 remained almost inactive during alkylation, which could be due to the small pore sizes. Similar microporous structure of HY restricted diffusion of the reactants and was responsible for incomplete conversion of 1-decene into alkylated product. HY also showed high shape-selectivity, resulting in 2-(2,4,6-trimethylphenyl)decane being the major component of reaction mixture at 86.8% (Fig. 16).

Recycling of the catalyst **1** resulted in decrease of activity, conversion of 1-decene was lower (51.6%) as compared to the initial alkylation reaction (90.3%). Presence of carbon deposits might have been responsible for partial pore blocking, thus leading to the poorer catalytic performance. This indicated the need for the future work regarding developing the optimum regeneration method to avoid loss of catalytic activity. However, changes in catalyst's characteristics were negligible. Slight decrease of BET surface area and insignificant acidity decrease was observed. Tungsten contents remained the same indicating that no PTA leaching took place during the reaction.

## *Conclusions*

A hybrid functionalized material containing phosphotungstic acid covalently embedded into a silica network was successfully synthesized by means of sol-gel method. The obtained mesoporous material had high BET surface area and high concentration of catalytically active surface acidic sites. Synthesized superacidic materials were effective in liquid-phase alkylation of 1,3,5-trimethylbenzene by 1-decene. Comparison of H-PTA/SiO<sub>2</sub> to well-known alkylation catalyst zeolite HY revealed higher activity of the former. Catalytic performance of obtained material was comparable to the activity of pure PTA in homogeneous catalysis. Analysis of the characteristics of the catalysts after alkylation showed that covalent incorporation of HPA clusters onto silica matrix prevented their leaching from the surface of the obtained material, thus enabling its regeneration and recycling.

## REFERENCES

- 1) Kocal, J., Vora, B., Imai, T. Production of linear alkylbenzenes. *Appl. Catal., A*. **2001**, 221, 295-301.
- 2) Webster-Gardiner, M., Chen, J., Vaughan, A., McKeown, B., Schinski, W., Gunnoe, T. Catalytic Synthesis of “Super” Linear Alkenyl Arenes Using an Easily Prepared Rh(I) Catalyst. *J. Am. Chem. Soc.* **2017**, 139, 5474-5480.
- 3) Benvenuto, M. *Industrial Organic Chemistry*. Walter de Gruyter GmbH: Berlin/Boston, **2017**.
- 4) GuoPeng, Q., Feng, J., XueWen S., SuoQi, Z. Alkylation Mechanism of Benzene with 1-Dodecene Catalyzed by Et<sub>3</sub>NHCl-AlCl<sub>3</sub>. *Chin. J. Chem.* **2010**, 53, 1102-1107.
- 5) Meriaudeau, P., Taarit, Y., Thangaraj, A., Almeida J.L.G., Naccache C. Zeolite Based Catalysts for Linear Alkylbenzene Production: Dehydrogenation of Long Chain Alkanes and Benzene Alkylation. *Catal. Today*. **1997**, 38, 243-247.
- 6) Wang, J-J., Chuang, Y-Y., Hsu, H-Y., Tsai, T-C. Toward Industrial Catalysis of Zeolites for Linear Alkylbenzene Synthesis: a Mini Review. *Catal. Today*. **2017**, 298, 109-116.
- 7) Zhao, Z., Qiao, W., Wang, G., Li, Z., Cheng, L. Alkylation of  $\alpha$ -Methylnaphthalene with Long-Chain Olefins Catalyzed by Rare Earth Lanthanum Modified HY Zeolite. *J. Mol. Catal. A: Chem.* **2006**. 250, 50-56.
- 8) Da, Z., Han, Z., Magnoux, P., Guisnet, M. Liquid-Phase Alkylation of Toluene with Long-Chain Alkenes over HFAU and HBEA Zeolites. *Appl. Catal. A: Chem.* **2001**, 219, 45-52.
- 9) Weitkamp, J. Zeolites and Catalysis. *Solid State Ionic.* **2000**, 131, 175-188.

- 10) Jeganathan, M., Pitchumani, K. Solvent-Free Synthesis of 1,5-Benzodiazepines Using HY Zeolite as a Green Solid Acid Catalyst. *ACS Sustain. Chem. Eng.* **2014**, 2, 1169-1176.
- 11) Kotrel, S., Knotziger, H., Gates, B.C. The Haag-Dessau Mechanism of Protolytic Cracking of Alkanes. *Microporous Mesoporous Mater.* **2000**, 11-20.
- 12) Blay, V., Louis, B., Miravalles, R., Yokoi, R., Peccatiello, K., Clough, M., Yilman, B. Engineering Zeolites for Catalytic Cracking to Light Olefin. *ASC Catalysis.* **2017**, 7, 6542-6566.
- 13) Hua, Z., Zhou, J., Shi, J. Recent Advances in Hierarchially Structured Zeolites: Synthesis and Material Performances. *Chem. Commun.* **2011**, 47, 10536-10547.
- 14) Awate, S.V., Waghmode, S.B., Agashe, M.S. Synthesis, Characterization and Catalytic Evaluation of Zirconia-Pillared Montmorillonite for Linear Alkylation of Benzene. *Catal. Commun.* **2004**, 5, 407-411.
- 15) Faghihian, H., Mohammadi, M.H. Surface Properties of Pillared Acid-Activated Bentonite as Catalysts for Selective Production of Linear Alkylbenzene. *Appl. Clay Sci.* **2013**, 264, 492-499.
- 16) Liu, Y., Zhou, Y., Sheng, X., Wang, B., Zhu, Z., Nan Q. The Catalytic Performance Study of Chloroaluminate Ionic Liquids on Long-Chain Alkenes Alkylation. *Energy Fuels.* **2018**, 32, 9, 9763-9771.
- 17) Xin, H., Wu, Q., Han, M., Wang, D., Jin, Y. Alkylation of Benzene with 1-Dodecene in Ionic Liquids  $[Rmim]^+Al_2Cl_6X^-$  (R=Butyl, Octyl and Dodecyl; X=chlorine, Bromine and Iodine). *Appl. Catal. A: Chem.* **2005**, 292, 354-361.

- 18) Qiao, K., Deng, Y. Alkylation of Benzene in Room Temperature Ionic Liquids Modified with HCl. *J. Mol. Catal. A: Chem.* **2001**, 171, 81-84.
- 19) He, Y., Zhang, Q., Zhan, X., Cheng, D., Chen, F. Aluminum Impregnated Silica Catalyst for Friedel-Crafts Reaction: Influence of Ordering Mesostructure. *Chinese J. Chem. Eng.* **2017**, 25, 1533-1538.
- 20) Kozhevnikov, I.V. Catalysis by Heteropoly Acids and Multicomponent Polyoxometalates in Liquid-Phase Reactions. *Chem. Rev.* **1998**, 98, 171-198.
- 21) Mizuno, N., Misono, M. Heterogeneous Catalysis. *Chem Rev.* **1998**, 98, 199-218.
- 22) Pinheiro, P.S., Rocha, A., Eon, J., Paiva Floro Bonfim, R., Sanches, S.G. Isomer Distribution in  $\alpha$ -Keggin Structures  $[XW_{12-n}V_nO_{40}]^{-(q+n)}$  X=Si, P( $0 \leq n \leq 4$ ): a DFT Study of Free Energy and Vibrational Spectra. *Comptes Rendus Chimie.* **2016**, 19, 1352-1362.
- 23) Kumar, G.S., Vishnuvarthan, M., Planichamy, M., Muugesan, V. SBA-15 Supported HPW: Effective Catalytic Performance in the Alkylation of Phenol. *J. Mol. Catal. A: Chem.* **2006**, 260, 49-55.
- 24) Wang, J., Zhu, H.O. Alkylation of 1-Dodecene with Benzene over  $H_3PW_{12}O_{40}$  Supported on Mesoporous Silica SBA-15. *Catal. Lett.* **2004**, 93, 209-212.
- 25) Ajakumar, S., Pandurangan, A. HPW and Supported HPW Catalyzed Condensation of Aromatic Aldehydes with Aniline: Synthesis of DATPM Derivatives. *J. Mol. Catal. A: Chem.* **2008**, 286, 21-30.
- 26) Zhang, W., Zhao, Q., Liu, T., Gao, Y., Li, Y., Zhang G., Zhang F., Fan, X. Phosphotungstic Acid Immobilized on Amine-Grafted Oxide as Acid/Base Bifunctional Catalyst for One-Pot Tandem Reaction. *Ind. Eng. Chem. Res.* **2014**, 53, 1437-1441.

- 27) Juan, J.C., Zhang, J.C., Yarmo, M.A. 12-Tungstophosphoric Acid Supported on MCM-41 for Esterification of Fatty Acids under Solvent-free Condition. *J. Mol. Catal. A: Chem.* **2007**, 276, 265-271.
- 28) Hoo, P.Y., Abdulah, A.Z. Direct Synthesis of Mesoporous 12-Tungstophosphoric Acid SBA-15 Catalyst for Selective Esterification of Glycerol and Lauric Acid to Monolaurate. *Chem. Eng. J.* **2014**, 250, 274-287.
- 29) Jermy, B.R., Pandurangam, A. H<sub>3</sub>PW<sub>12</sub>O<sub>40</sub> Supported on MCM-41 Molecular Sieves: an Effective Catalyst for Acetal Formation. *Appl. Catal. A: Gen.* **2005**, 295, 185-192.
- 30) Okuhara, T., Nishimura, T., Misono, M. Novel Microporous Solid "Superacids": Cs<sub>x</sub>H<sub>3-x</sub>PW<sub>12</sub>O<sub>40</sub> (2 ≤ x ≤ 3). In: *Studies in Surface Science and Catalysis*, Hightower, J.W., Delgass, W.N., Iglesia, E., Bell, A.T. (Eds.). Elsevier, Amsterdam. **1996**, 101, 581-590.
- 31) Dafaud, V., Lefebvre, F. Inorganic Hybrid Materials with Encapsulated Polyoxometalates. *Materials.* **2010**, 3, 682-703.
- 32) Yang, L., Qi, Y., Yuan, X., Shen, J., Kim, J. Direct Synthesis, Characterization and Catalytic Application of SBA-15 Containing Heteropolyacid H<sub>3</sub>PW<sub>12</sub>O<sub>40</sub>. *J. Mol. Catal. A: Chem.* **2005**, 229, 199-205.
- 33) Shi, C., Wang, R., Zhu, G., Qiu, S., Long, J. Synthesis, Characterization, and Catalytic Properties of SiPW-X mesoporous Silica with Heteropolyacids Encapsulated into Their Framework. *Eur. J. Inorg. Chem.* **2005**, 4801-4807.
- 34) Adetola, O., Little, I., Mohseni, R., Molodyi, D., Bohvan, S., Golovko, L., Vasiliev, A. Synthesis of Mesoporous Silica Gel with Embedded Heteropolyacids. *J. Sol-Gel Sci. Technol.* **2017**, 81, 205-213.
- 35) Brinker, C.J., Scherer, G.W. Sol-Gel Science. Academic Press: London. **1990**.



- 36) Nakanishi, T., Norisuye, T., Sato, H., Takemori, T., Tran-Cong-Miyata, Q., Sugimoto, T., Nomura, S. Studies of Microscopic Structure of Sol-Gel Derived Nanohybrids Containing Heteropolyacids. *Macromolecules*. **2007**, 40, 4165-4172.
- 37) Buckley, A.M., Greenblatt, M. The Sol-Gel Preparation of Silica Gels. *J. Chem. Edu.* **1994**, 71, 599-602.
- 38) Dubey, R.S., Rajesh, Y.B.R., More, M.A. Synthesis and Characterization of SiO<sub>2</sub> Nanoparticles via Sol-Gel Method for Industrial Application. *Mater. Today-Proc.* **2015**, 2, 3575-3579.
- 39) Bogush, G.H., Zukoski, C.F. Studies of the Kinetics of the Precipitation of Uniform Silica Particles through the Hydrolysis and Condensation of Silicon Alkoxides. *J. Colloid Interface Sci.* **1991**, 142, 1-18.
- 40) Singh, L.P., Bhattacharyya, S.K., Kumar, R., Mishra, G., Sharma, U, Singh G., Ahalawat, S. Sol-Gel Processing of Silica Nanoparticles and their Application. *Adv. Colloid Interface Sci.* **2014**, 214, 17-37.
- 41) Wang, L., Ding, W., Sun, Y. The Preparation and Application of Mesoporous Materials for Energy Storage. *Mater. Res. Bull.* **2015**, 83, 230-249.
- 42) Wingen, A., Kleitz, F., Schuth, F. Ordered Mesoporous Materials: Preparation and Application in Catalysis. In: *Basic Principles in Applied Catalysis*, Baerns, M. (Ed.), Springer, Berlin. **2004**, 75, 281-319.
- 43) Shen, S.C., Ng, W., Chia, L.S., Dong, Y.C., Tan, R.B. Applications of Mesoporous Materials as Excipients for Innovative Drug Delivery and Formulation. *Curr. Pharm. Des.* **2013**, 19, 6270-6289.

- 44) Bajpai, P. *Recycling and Deinking of Recovered Paper*. Elsevier Science Publishing Co: Amsterdam. **2013**.
- 45) Seaton, K., Little, I., Tate, C., Mohseni, R., Roginskaya, M., Povazhniy, V., Vasiliev, A. Adsorption of Cesium on Silica Gel Containing Embedded Phosphotungstic Acid. *Microporous Mesoporous Mater.* **2017**, 244, 55-66.
- 46) Marosi, L., Platero, E.E., Cifre, J., Arean, C.O. Thermal Dehydration of  $H_{3+x}PV_xM_{12-x}O_{40} \cdot yH_2O$  Keggin Type Heteropolyacids; Formation, Thermal Stability and Structure of the Anhydrous Acids  $H_3PM_{12}O_{40}$ , of the Corresponding Anhydrides  $PM_{12}O_{38.5}$  and of a Novel Trihydrate  $H_3PW_{12}O_{40} \cdot 3H_2O$ . *J. Mater. Chem.* **2000**, 10, 1949-1955.
- 47) Okuhara, T., Noritaka, M., Lee, K.Y., Misono, M. Catalysis by Heteropoly Compounds. XIII. An Infrared Study of Ethanol and Diethyl Ether in the Pseudoliquid Phase of 12-Tungstophoric Acid. *Bull. Chem. Soc. Jpn.* **1989**, 62, 1731-1739.
- 48) Jörke, A., Kohls, E., Triemer, S., Seigel-Morgenstern, A., Hamel, C., Stein, M. Resolution of Structural Isomers of Complex Reaction Mixtures in Homogeneous Catalysis. *Chem. Eng. Process Process Intensif.* **2016**, 102, 229-237.
- 49) Okuhara, T., Tatematsu, S., Lee, K.Y., Misono, M. Catalysis by Heteropoly Compounds. XII. Absorption Properties of 12-Tungstophosphoric Acid and its Salts. *Bull. Chem. Soc. Jpn.* **1989**, 62, 717-723.
- 50) Holclajtner-Antunović, I., Bajuk-Bogdanović, D., Todović, M., Mioć, U.B., Zakrazewska, J., Uskoković-Marković, S. pH-Dependent Interactions between Keggin Heteropolyanions in Dilute Solutions. *Can. J. Chem.* **2008**, 86, 996-1004.

- 51) Okuhara, T., Nishimura, T., Watanabe, H., Misono, M. Insoluble Heteropoly Compounds as Highly Active Catalysts for Liquid-Phase Reactions. *J. Mol. Catal.* **1992**, 74, 247-256.
- 52) Jewett, J. R., Jensen, L. Assessment of Available Particle Size Data to Support an Analysis of Waste Feed Delivery System Transfer System. Report RPP-6247. US Department of Energy. Washington, DC. **2000**.
- 53) Deshmukh, A.R.A.S., Gumaste, V.K., Bhawal, B.M. Alkylation of Benzene with Long Chain (C8-C18) linear Primary Alcohols over Zeolite-Y. *Catal. Lett.* **2000**, 64, 247-250.
- 54) Dimitratos, N., Védrine, J.C. Properties of Cs<sub>2.5</sub> Salts of Transition Metal M Substituted Keggin-type M<sub>1-x</sub>PV<sub>1</sub>Mo<sub>11-x</sub>O<sub>40</sub> Heteropolyoxometallates in Propane Oxidation. *Appl. Catal. A: Gen.* **2003**, 256, 251-263.
- 55) Hanif M.A., Nisar, S., Rashid, U. Supported Solid and Heteropolyacid Catalysts for Production of Biodiesel. *Catal. Rev.* **2017**, 59, 165-188.
- 56) Okuhara, T., Watanabe, H., Nishimura, T., Inumaru, K., Misono, M. Microstructure of cesium Hydrogen Salts of 12-Tungstophosphoric Acid Relevant to Novel Acid Catalysis. *Chem. Mater.* **2000**, 12, 2230-2238.

## VITA

### ANASTASIA KUVAYSKAYA

- Education: M.A. Chemistry, East Tennessee State University, Johnson City, Tennessee, 2020  
B.S. Chemistry, East Tennessee State University, Johnson City, Tennessee, 2018  
B.A. Linguistics, Kursk State University, Kursk, Russia, 2006
- Professional Experience: Teacher, Kursk Middle School; Kursk, Russia, 2005-2006  
Graduate Assistant, East Tennessee State University, College of Arts and Sciences, 2018-2020
- Publications: Kuvayskaya A., Vasiliev A. Functionalization of Silica Gel by Ultrasound-assisted Surface Suzuki Coupling. *Tetrahedron Lett.* **2019**, 60 (37): 150937  
Kuvayskaya A., Garcia, S., Mohseni, R., Vasiliev, A. Superacidic Mesoporous Catalysts Containing Embedded Heteropolyacids. *Catal. Lett.* **2019**, 149: 1983-1990
- Presentations: **Kuvayskaya, A., Vasiliev, A.** Immobilized Phosphotungstic Acid For Low-waste Catalytic Alkylation of Aromatic Compounds. *Eastman-NETSACS Student Research Symposium*. Kingsport, TN, 2019.  
**Kuvayskaya, A., Vasiliev, A.** Low-waste Synthesis of Long-Chain Alkylbenzenes on Superacidic Mesoporous Catalysts. *The 71<sup>st</sup> Southeastern Regional Meeting of American Chemical Society*. Savannah, GA, 2019.  
**Kuvayskaya, A., Lotsi, B., Mohseni, R., Vasiliev., A.** Mesoporous Adsorbents for Perfluorinated Compounds. U.S. *EPA's 15<sup>th</sup> Annual People, Prosperity and Planet (P3) National Sustainable Student Design Competition*. TechConnect World Innovation Conference and Expo. Boston, MA, 2019  
**Kuvayskaya, A., Garcia, S., Vasiliev, A.** Low-waste Synthesis of Long-chain Alkylbenzenes. *23<sup>rd</sup> Green Chemistry and Engineering Conference/9<sup>th</sup> International Conference in Green and Sustainable Chemistry*. Reston, VA, 2019  
**Kuvayskaya, A., Vasiliev, A.** Use of Suzuki Coupling Reaction for Synthesis of Functionalized Materials. *Appalachian Student*

*Research Forum*. East Tennessee State University, Johnson City, TN, 2019

**Kuvayskaya, A.**, Garcia, S., Vasiliev, A. Synthesis of Long-chain Alkylbenzenes on Superacidic Catalysts Containing Embedded Phosphotungstic Acid. *Appalachian Student Research Forum*. East Tennessee State University, Johnson City, TN, 2019

**Kuvayskaya, A.**, Vasiliev, A. Modification of Silica Surface by Suzuki Coupling. *257<sup>th</sup> ACS Spring National Meeting And Exposition*. Orlando, FL, 2019, COLL 154

Kuvayskaya, A., Garcia, S., **Vasiliev, A.** Superacidic Mesoporous Catalysts of Alkylation of Aromatic Compounds. *257<sup>th</sup> ACS Spring National Meeting and Exposition*. Orlando, FL, 2019, CATL 606.

**Kuvayskaya, A.**, Vasiliev, A. Synthesis of Long-chain Alkylbenzenes on Heterogeneous Superacidic Catalysts. *The 128<sup>th</sup> Meeting of Tennessee Academy of Science*. Austin Peay University, Clarksville, TN, 2018. Abstr. publ. in: *Journal of Tennessee Academy of Science* 2019, 94: 17.

**Kuvayskaya, A.**, Vasiliev, A. Heterogeneous Superacidic Catalysts Containing Immobilized Heteropolyacids. *The 70<sup>th</sup> Southeastern Regional Meeting of American Chemical Society*. Augusta, GA, 2018. Abstr. 247.

\*presenters identified in bold

Honors and Awards:

Outstanding Teaching Assistant Award, East Tennessee State University, 2018-2019

3<sup>rd</sup> Place in Oral Presentation, the 128<sup>th</sup> Meeting of Tennessee Academy of Science, 2018

1<sup>st</sup> Place Prize in Master's Group 1 Physical and Chemical Sciences Oral Presentation, 2019 Appalachian Student Research Forum

3<sup>rd</sup> Place in Poster Presentation, 2019 Eastman-NETSACS Student Research Symposium

Grants Received:

Kuvayskaya A. and Vasiliev A. Student Faculty Collaborative Grant. ETSU/Honors College.

Kuvayskaya A. and Vasiliev A. American Chemical Society Petroleum Research Fund 58891-UR5. ACS-PRF.